



Quantum perspectives in computing, sensing, communication, and metrology

Edoardo Charbon

EPFL

EPFL, Lausanne, Switzerland

Acknowledgements

Simone Frasca

Pascal 't Hart

Jiang Gong

Harald Homulle

Andrea Ruffino

Yatao Peng

M. Fernando Gonzalez-Zalba

Fabio Sebastiano

Masoud Babaie

Daniele Faccio

Andrew Dzurak

Outline

1. Quantum computing (2 periods)
2. Cryogenic electronics (2 periods)

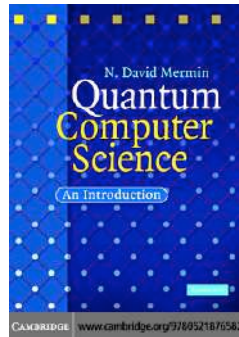
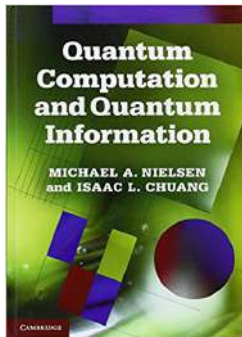
Available in a future class:

3. Quantum algorithms (2 periods)
4. Quantum imaging and communications (1 period)
5. Quantum metrology (2 periods)



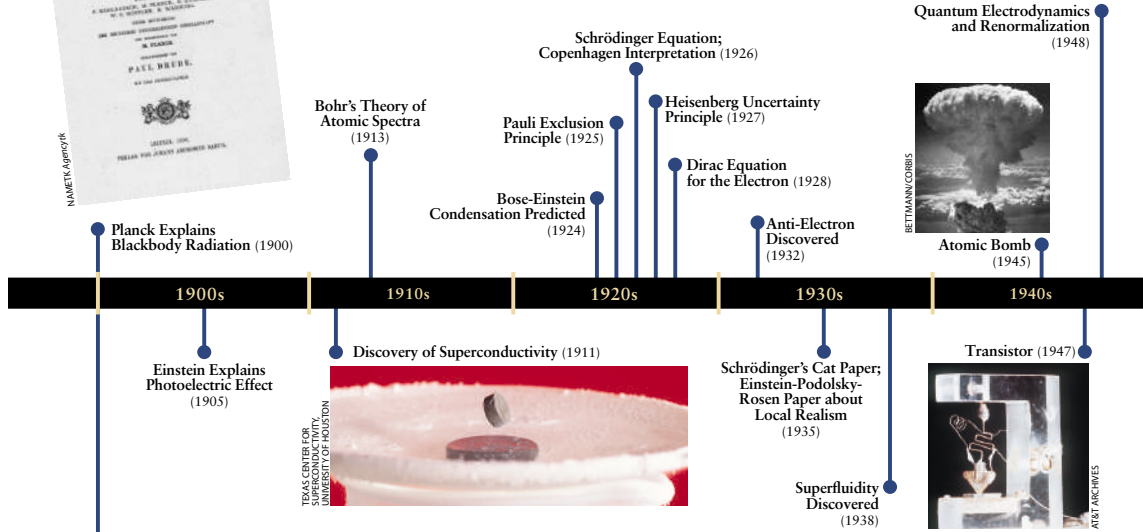
1. Quantum Computing

Suggested Reading

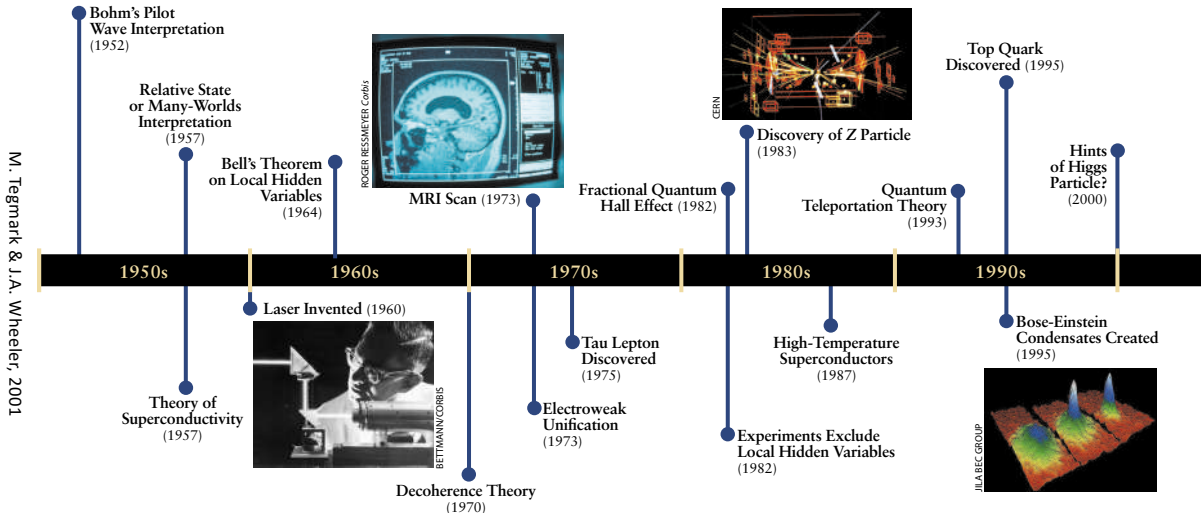


The First Quantum Revolution

M. Tegmark & J.A. Wheeler, 2001



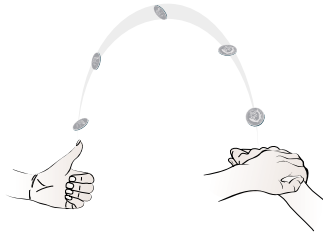
The First Quantum Revolution



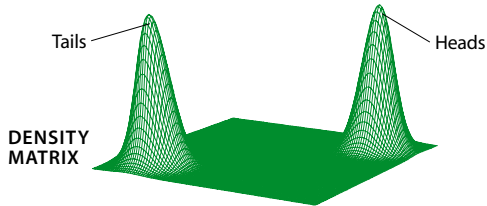
Weird Quantum Properties: Superposition & Entanglement

Superposition

CLASSICAL UNCERTAINTY



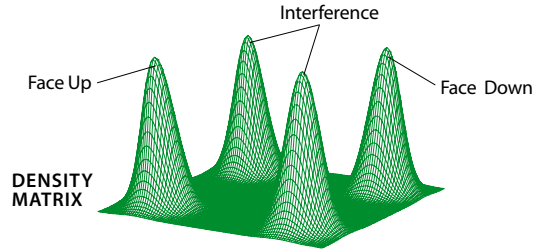
COIN TOSS



QUANTUM UNCERTAINTY

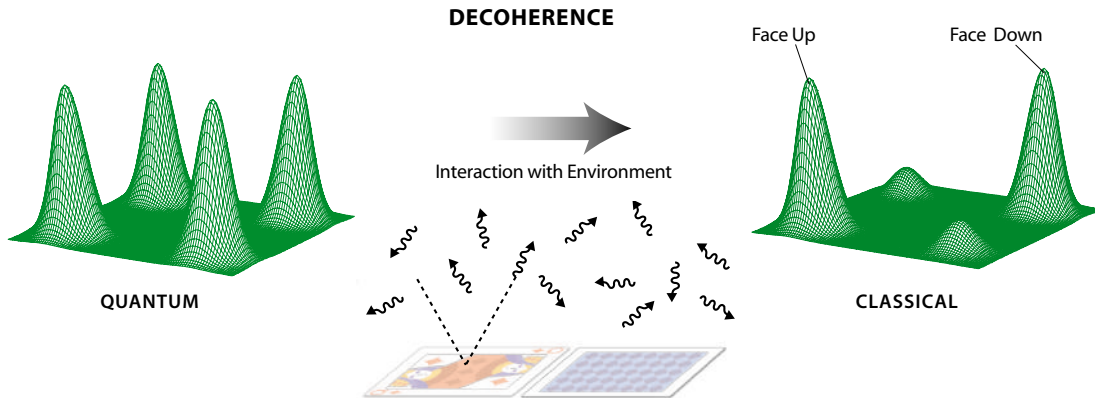


COHERENT SUPERPOSITION



Coherence / Decoherence

M. Tegmark & J.A. Wheeler, 2001



Entanglement

Definition: two particles are entangled if the quantum state of one particle cannot be described independently from the quantum state of the other particle.

Intuition: measuring the quantum state of one particle implies knowledge of the quantum state (e.g. momentum, spin, polarization, etc.) of the other entangled particle using the same projection.

The Second Quantum Revolution

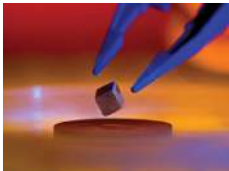
- Spearheaded by many, *in primis* Richard Feynman
- Proposal to use of **entanglement** and **superposition** for computation
- Fundamentals and theory developed in the 1980-2000s

There is plenty of space at the bottom

- Richard Feynman



The Promise of Quantum Computing



Energy

Room-temperature
superconductivity



Health

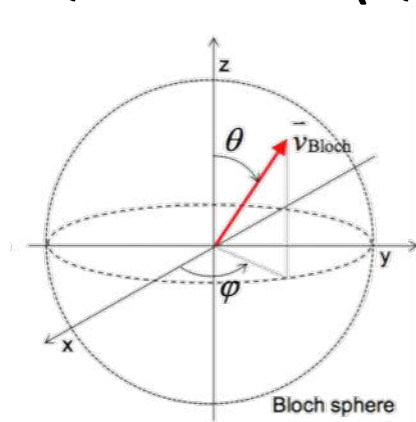
Quantum chemistry



Internet Security

Source: L. Vandersypen, ISSCC 2017

Quantum Bit (Qubit)



$$|\psi\rangle = \alpha_0|0\rangle + \alpha_1|1\rangle$$

- Superposition
- Entanglement

The Power of Superposition

1 qubit.....2 states

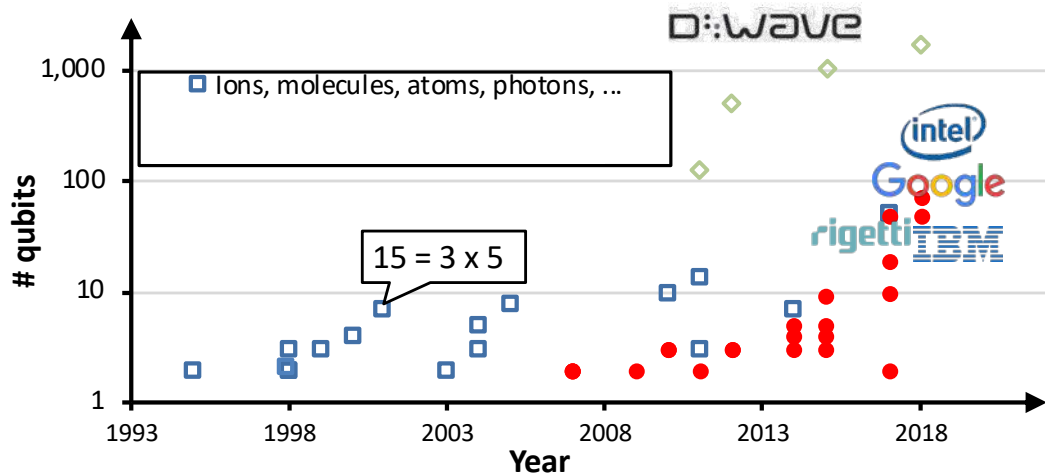
2 qubits.....4 states

N qubits..... 2^N states

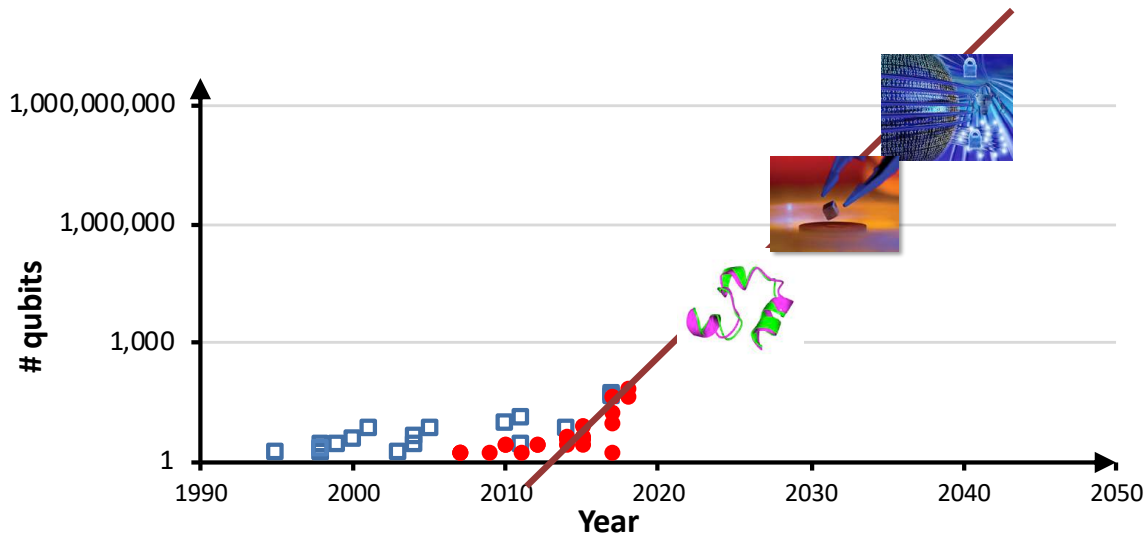
40 qubits: 10^{12} parallel operations

300 qubits: more than the atoms in the universe

State-of-the-Art



How Far Are We from Something Useful?



Quantum Supremacy or Quantum Advantage

Quantum supremacy is the potential ability of quantum computing devices to solve problems that classical computers practically cannot.

[Wikipedia]

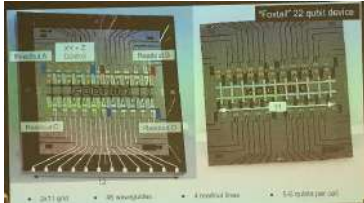
Google claims to have reached quantum supremacy (Financial Times)

Report on a an accepted paper to a peer-reviewed publication

Solid-state Qubit Implementations Today

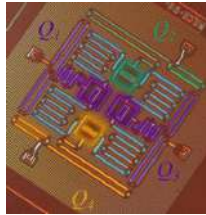
- Based on superconducting qubits
- First multi-qubit chips announced
- Freely available qubits on line

72-qubit chip announced



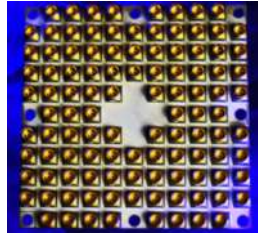
Source: Tristan Meunier

16 Qubits online version

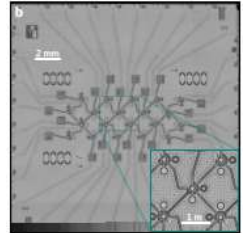


50 qubit chip
announced

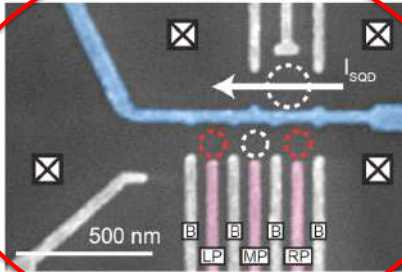
49 qubit chip



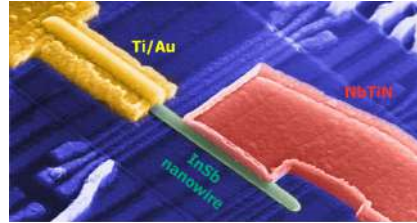
19 qubit chip



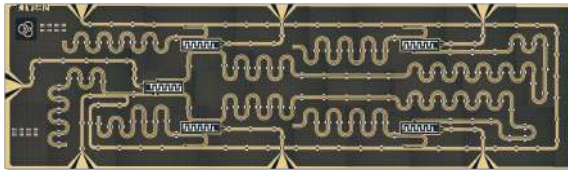
Solid-state Qubit Implementations Today



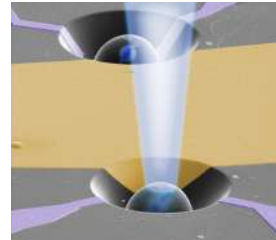
Semiconductor quantum dots



Semiconductor-superconductor hybrids



Superconducting circuits



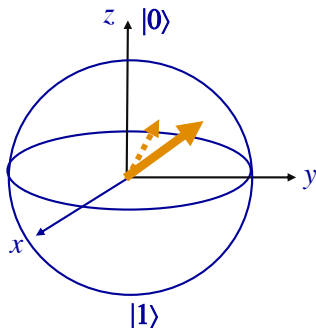
Impurities in diamond or silicon

Source: L. Vandersypen, 2017

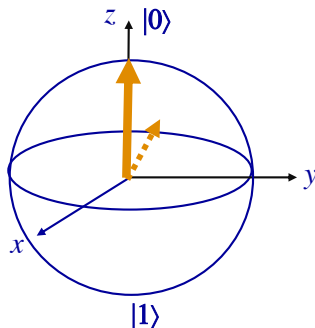
Qubits are Fragile

- Environment can cause decoherence due to dephasing and relaxation
- Fidelity

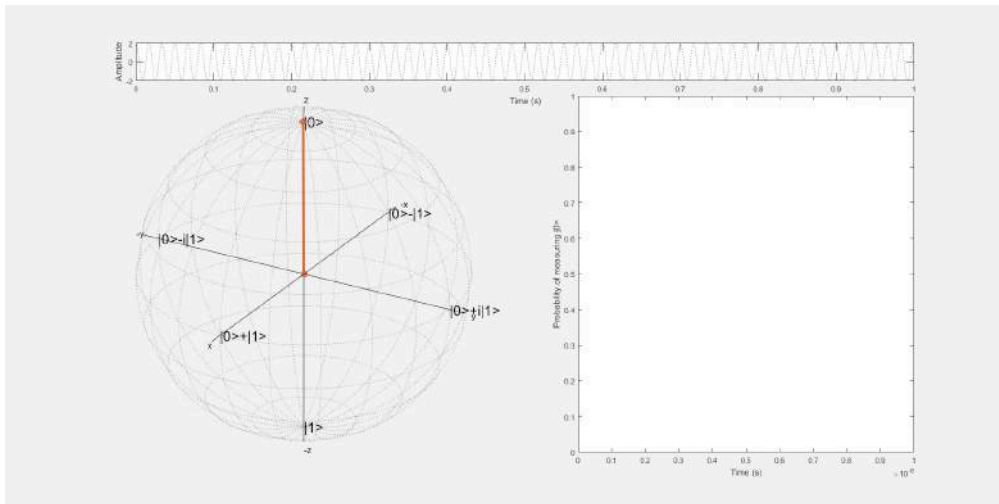
Dephasing



Relaxation



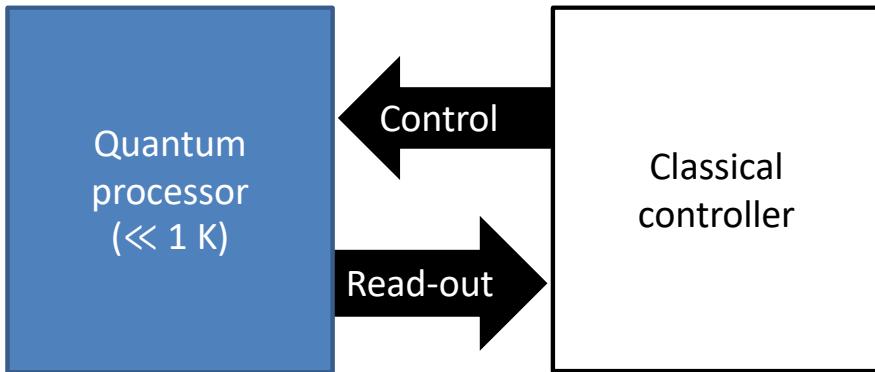
Qubit Transition from $|0\rangle$ to $|1\rangle$



© Jeroen van Dijk

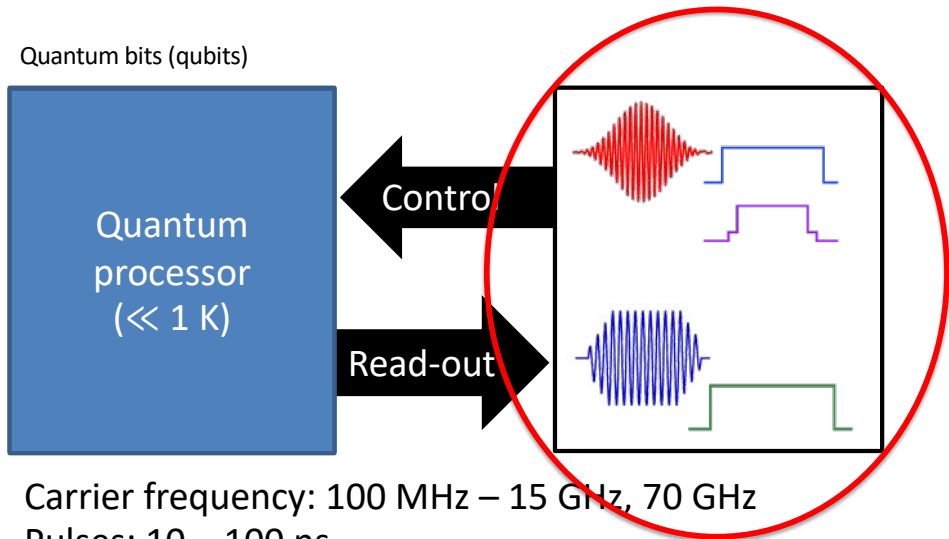
Interfacing Qubits with Classical World

Quantum bits (qubits)



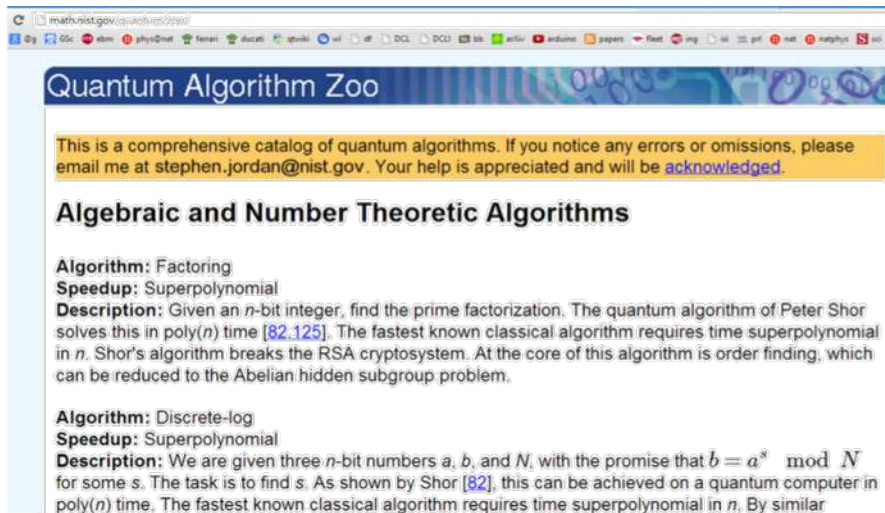
- Carrier frequency: 100 MHz – 15 GHz, 70 GHz
- Pulses: 10 – 100 ns

Interfacing Qubits with Classical World



- Carrier frequency: 100 MHz – 15 GHz, 70 GHz
- Pulses: 10 – 100 ns
- Readout techniques for spin qubits: **ESR, EDSR**

Status of Quantum Algorithms



The screenshot shows a web browser window with the address bar displaying `math.nist.gov/quantum/zoo/`. The browser's toolbar includes various icons for search engines and social media. The website's header features the title "Quantum Algorithm Zoo" in a blue banner. Below the header, a yellow box contains a message from Stephen Jordan at NIST, inviting users to report errors or omissions. The main content area is titled "Algebraic and Number Theoretic Algorithms" and lists two algorithms: Factoring and Discrete-log. Each algorithm entry includes its name, a speedup claim, and a detailed description of the problem and the quantum algorithm's advantage over classical methods.

math.nist.gov/quantum/zoo/

Quantum Algorithm Zoo

This is a comprehensive catalog of quantum algorithms. If you notice any errors or omissions, please email me at stephen.jordan@nist.gov. Your help is appreciated and will be [acknowledged](#).

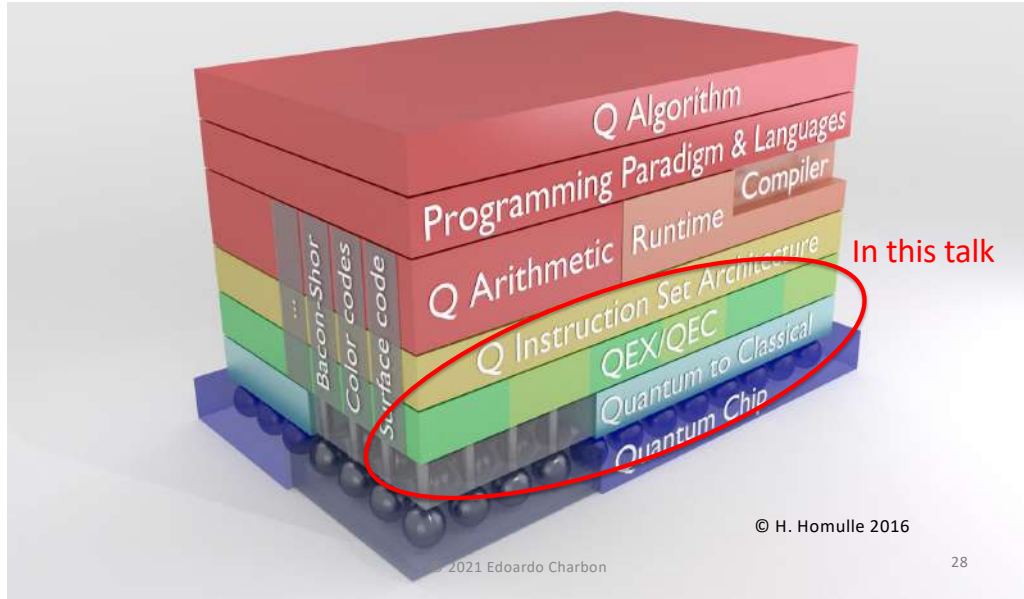
Algebraic and Number Theoretic Algorithms

Algorithm: Factoring
Speedup: Superpolynomial
Description: Given an n -bit integer, find the prime factorization. The quantum algorithm of Peter Shor solves this in $\text{poly}(n)$ time [82,125]. The fastest known classical algorithm requires time superpolynomial in n . Shor's algorithm breaks the RSA cryptosystem. At the core of this algorithm is order finding, which can be reduced to the Abelian hidden subgroup problem.

Algorithm: Discrete-log
Speedup: Superpolynomial
Description: We are given three n -bit numbers a , b , and N , with the promise that $b = a^s \pmod N$ for some s . The task is to find s . As shown by Shor [82], this can be achieved on a quantum computer in $\text{poly}(n)$ time. The fastest known classical algorithm requires time superpolynomial in n . By similar

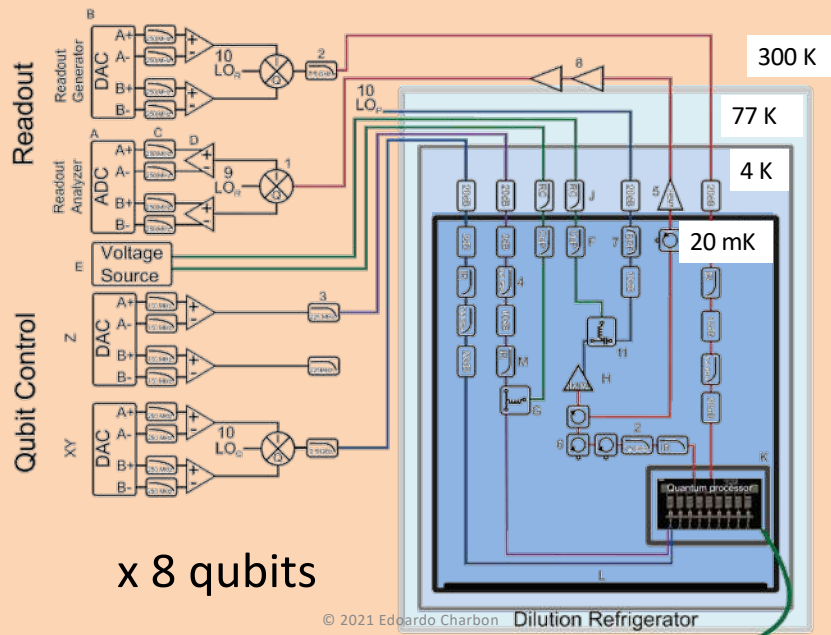
~50 algorithms with quantum speedup, but most people know 2.

Quantum Computing Stack



Quantum Computer Architecture

A Real-life Quantum Computer



Today's Solution

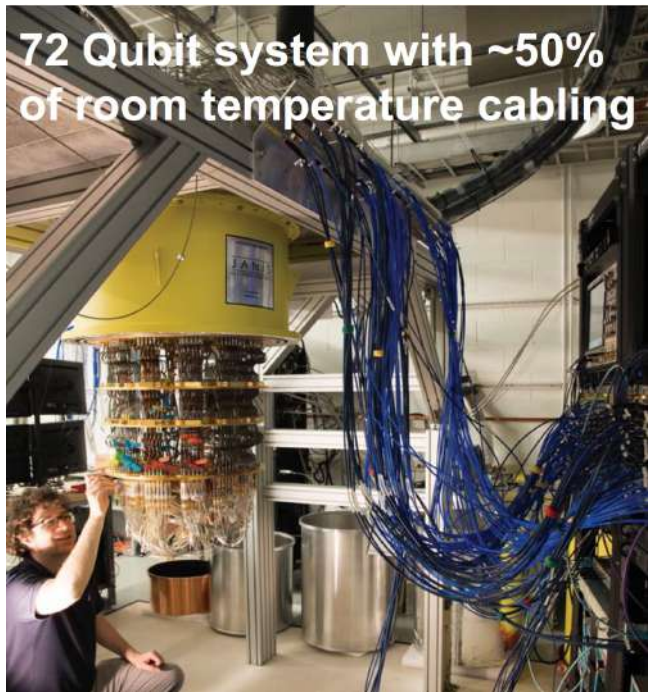
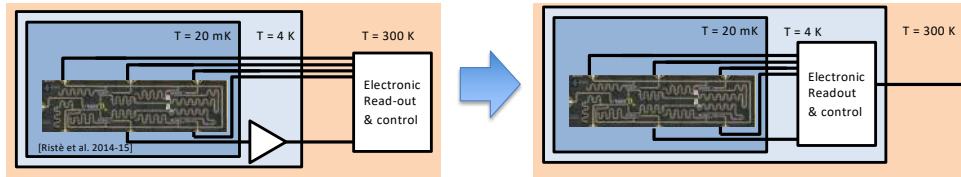


Image: Google Bristlecone. Taken from: J.C. Bardin et al.,
"An Introduction to Quantum Computing for RFIC
Engineers", RFIC Symposium 2019

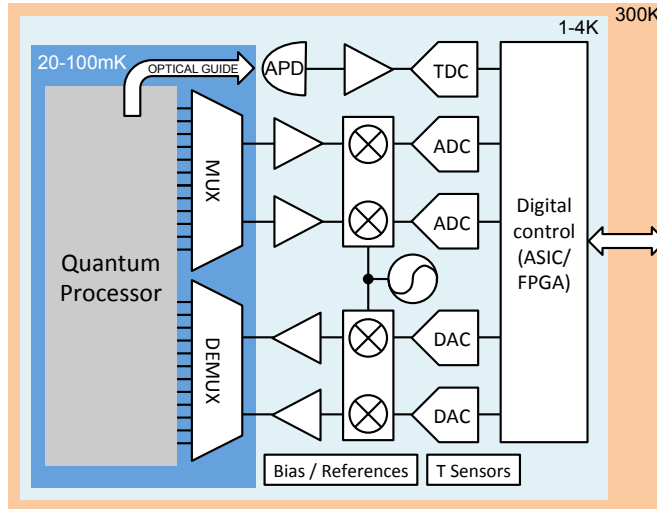
Our Proposed Solution

- **Proposed solution**
 - Electronics at 4 K
 - Only connections to 4 K to 20 mK are needed



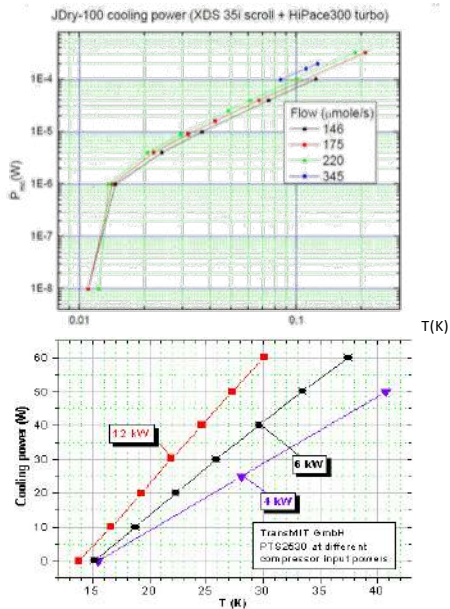
- **Ultimate solution**
 - Qubits at 4 K
 - Monolithic integration

Electronic Readout & Control



E. Charbon *et al.*, *IEDM* 2016

Cooling Power Issue



Dilution refrigerator



300 K

70 K

4 K

100 mK

20 mK

Courtesy: Oxford instruments

Scalability Issue

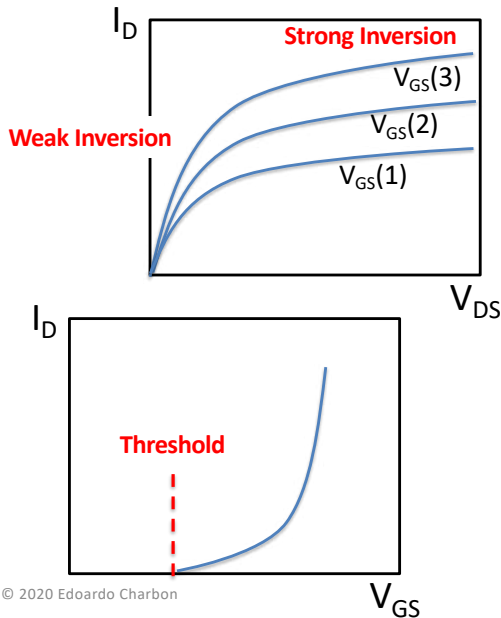
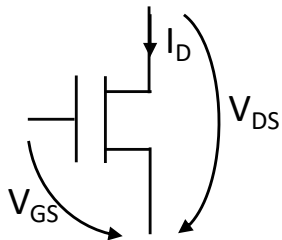
- Noise budget..... $< 0.1\text{nV}/\text{VHz}$
- Power budget (for scalability)..... $\ll 2\text{mW}/\text{qubit}$
- Physical dimensions (for scalability)..... 30nm
- Bandwidth (for multiplexing)..... $1\text{-}12\text{GHz}$
- Kick-back avoidance

2. Cryogenic Electronics

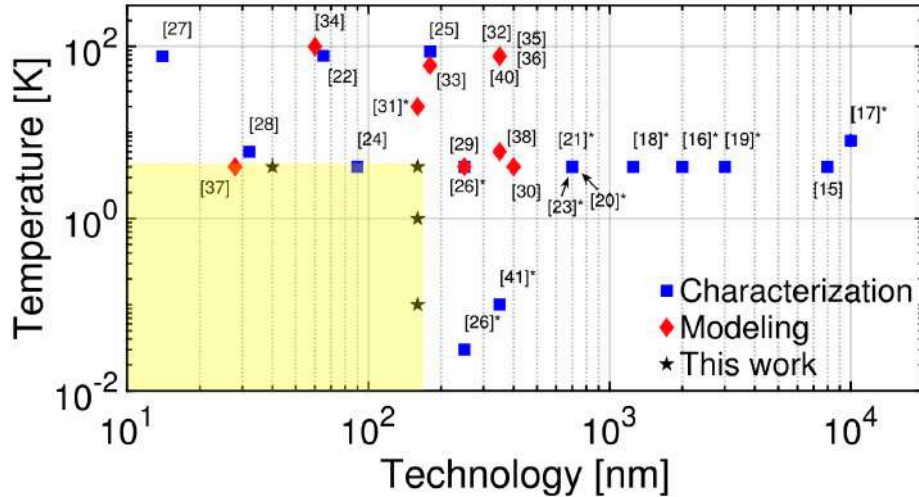
Transistor Modeling at Deep Cryogenic Temperatures

CMOS Modeling: Important Parameters

- MOSFET



CMOS Modeling: History



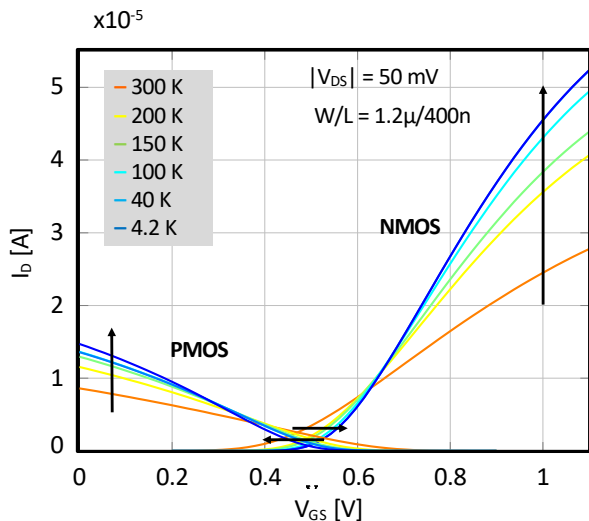
R.M. Incandela et al., *ESSDERC* 2017

R.M. Incandela et al., *J. of EDS* 2018

- [16] H. Hanamura *et al.*, "Operation of bulk CMOS devices at very low temperatures," *IEEE J. Solid-State Circuits*, vol. 21, no. 3, pp. 484–490, Jun. 1986, doi: [10.1109/JSSC.1986.1052555](#).
- [17] F. Balestra, L. Audaire, and C. Lucas, "Influence of substrate freeze-out on the characteristics of MOS transistors at very low temperatures," *Solid State Electron.*, vol. 30, no. 3, pp. 321–327, Mar. 1987, doi: [10.1016/0038-1101\(87\)90190-0](#).
- [18] L. Deferm, E. Simoen, and C. Claeys, "The importance of the internal bulk-source potential on the low temperature kink in NMOSTs," *IEEE Trans. Electron Devices*, vol. 38, no. 6, pp. 1459–1466, Jun. 1991, doi: [10.1109/16.81639](#).
- [19] E. Simoen, B. Dierickx, and C. L. Claeys, "Low-frequency noise behavior of Si NMOSTs stressed at 4.2 K," *IEEE Trans. Electron Devices*, vol. 40, no. 7, pp. 1296–1299, Jul. 1993, doi: [10.1109/16.216435](#).
- [20] E. Simoen and C. Claeys, "Impact of CMOS processing steps on the drain current kink of NMOSFETs at liquid helium temperature," *IEEE Trans. Electron Devices*, vol. 48, no. 6, pp. 1207–1215, Jun. 2001, doi: [10.1109/16.925249](#).
- [21] E. Simoen *et al.*, "Impact of irradiations performed at liquid helium temperatures on the operation of 0.7 μm CMOS devices and read-out circuits," in *Proc. Radiat. Effects Compon. Syst. (RADECS)*, 2003, pp. 369–375.
- [22] A. Siligaris *et al.*, "High-frequency and noise performances of 65-nm MOSFET at liquid nitrogen temperature," *IEEE Trans. Electron Devices*, vol. 53, no. 8, pp. 1902–1908, Aug. 2006, doi: [10.1109/TED.2006.877872](#).
- [23] Y. Creten, P. Merken, W. Sansen, R. Mertens, and C. van Hoof, "A cryogenic ADC operating down to 4.2K," in *IEEE Int. Solid-State Circuits Conf. Dig. Tech. Papers*, San Francisco, CA, USA, Feb. 2007, pp. 468–616, doi: [10.1109/ISSCC.2007.373497](#).
- [24] S.-H. Hong *et al.*, "Low-temperature performance of nanoscale MOSFET for deep-space RF applications," *IEEE Electron Device Lett.*, vol. 29, no. 7, pp. 775–777, Jul. 2008, doi: [10.1109/LED.2008.2000614](#).
- [25] G. De Geronimo *et al.*, "Front-end ASIC for a liquid argon TPC," in *Proc. IEEE Nuclear Sci. Symp. Med. Imag. Conf.*, vol. 58, Knoxville, TN, USA, Oct. 2010, pp. 1658–1666, doi: [10.1109/NSSMIC.2010.5874057](#).
- [26] S. R. Ekanayake, T. Lehmann, A. S. Dzurak, R. G. Clark, and A. Brawley, "Characterization of SOS-CMOS FETs at low temperatures for the design of integrated circuits for quantum bit control and readout," *IEEE Trans. Electron Devices*, vol. 57, no. 2, pp. 539–547, Feb. 2010, doi: [10.1109/TED.2009.2037381](#).
- [27] M. Shin *et al.*, "Low temperature characterization of 14nm FDSOI CMOS devices," in *Proc. 11th Int. Workshop Low Temp. Electron. (WOLTE)*, Grenoble, France, Jul. 2014, pp. 29–32, doi: [10.1109/WOLTE.2014.6881018](#).
- [28] A. H. Coskun and J. C. Bardin, "Cryogenic small-signal and noise performance of 32nm SOI CMOS," in *Proc. IEEE MTT-S Int. Microw. Symp. (IMS)*, Tampa, FL, USA, Jun. 2014, pp. 1–4, doi: [10.1109/MWSYM.2014.6848614](#).
- [29] Y. Feng, P. Zhou, H. Liu, J. Sun, and T. Jiang, "Characterization and modelling of MOSFET operating at cryogenic temperature for hybrid superconductor-CMOS circuits," *Semicond. Sci. Technol.*, vol. 19, no. 12, pp. 1381–1385, Oct. 2004, doi: [10.1088/0268-1242/19/12/009](#).
- [30] A. Akturk *et al.*, "Impact ionization and freeze-out model for simulation of low gate bias kink effect in SOI-MOSFETs operating at liquid He temperature," in *Proc. Conf. Simulat. Semicond. Process. Devices (SISPAD)*, Sep. 2009, pp. 1–4, doi: [10.1109/SISPAD.2009.5290227](#).
- [31] A. Akturk *et al.*, "Compact and distributed modeling of cryogenic bulk MOSFET operation," *IEEE Trans. Electron Devices*, vol. 57, no. 6, pp. 1334–1342, Jun. 2010, doi: [10.1109/TED.2010.2046458](#).
- [32] Z. Zhu *et al.*, "Design applications of compact MOSFET model for extended temperature range (60–400 K)," *Electron. Lett.*, vol. 47, no. 2, pp. 141–142, Jan. 2011, doi: [10.1049/el.2010.3468](#).
- [33] P. Martin, A. S. Royet, F. Guellec, and G. Ghibaudo, "MOSFET modeling for design of ultra-high performance infrared CMOS imagers working at cryogenic temperatures: Case of an analog/digital 0.18 μm CMOS process," *Solid-State Electron.*, vol. 62, no. 1, pp. 115–122, 2011, doi: [10.1016/j.sse.2011.01.004](#).
- [34] Z. Chen, H. Wong, Y. Han, S. Dong, and B. L. Yang, "Temperature dependences of threshold voltage and drain-induced barrier lowering in 60 nm gate length MOS transistors," *Microelectron. Rel.*, vol. 54, nos. 6–7, pp. 1109–1114, Jun./Jul. 2014, doi: [10.1016/j.microrel.2013.12.005](#).
- [35] H. Zhao and X. Liu, "Modeling of a standard 0.35 μm CMOS technology operating from 77K to 300K," *Cryogenics*, vol. 59, pp. 49–59, Jan. 2014, doi: [10.1016/j.cryogenics.2013.10.003](#).
- [36] G. S. Fonseca, L. B. de Sá, and A. C. Mesquita, "Extraction of static parameters to extend the EKV model to cryogenic temperatures," in *Proc. SPIE Defense Security*, Baltimore, MD, USA, May 2016, Art. no. 98192B, doi: [10.1117/12.2219734](#).
- [37] A. Beckers *et al.*, "Cryogenic characterization of 28 nm bulk CMOS technology for quantum computing," in *Proc. 47th Eur. Solid-State Device Res. Conf. (ESSDERC)*, Leuven, Belgium, Sep. 2017, pp. 62–65, doi: [10.1109/ESSDERC.2017.8066592](#).
- [38] N. C. Dao *et al.*, "An enhanced MOSFET threshold voltage model for the 6–300 K temperature range," *Microelectron. Rel.*, vol. 69, pp. 36–39, Feb. 2017, doi: [10.1016/j.microrel.2016.12.007](#).
- [39] R. M. Incandela *et al.*, "Nanometer CMOS characterization and compact modeling at deep-cryogenic temperatures," in *Proc. 47th Eur. Solid-State Device Res. Conf. (ESSDERC)*, Leuven, Belgium, Sep. 2017, pp. 58–61, doi: [10.1109/ESSDERC.2017.8066591](#).
- [40] L. Varizat, G. Sou, M. Mansour, D. Alison, and A. Rhouni, "A low temperature 0.35 μm CMOS technology BSIM3.3 model for space instrumentation: Application to a voltage reference design," in *Proc. IEEE Int. Workshop Metrol. AeroSpace (MetroAeroSpace)*, Padua, Italy, Jun. 2017, pp. 74–78, doi: [10.1109/MetroAeroSpace.2017.7999541](#).
- [41] A. Rhouni *et al.*, "First-ever test and characterization of the AMS standard bulk 0.35 μm CMOS technology at sub-Kelvin temperatures," *J. Phys. Conf. Series*, vol. 834, no. 1, May 2017, Art. no. 012005, doi: [10.1088/1742-6596/834/1/012005](#).

R.M. Incandela et al., *J. of EDS* 2018

What Happens to CMOS at Cryo?

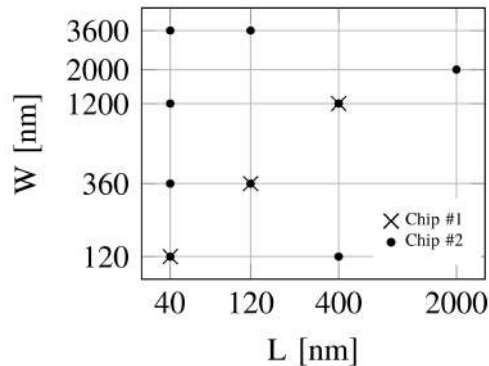
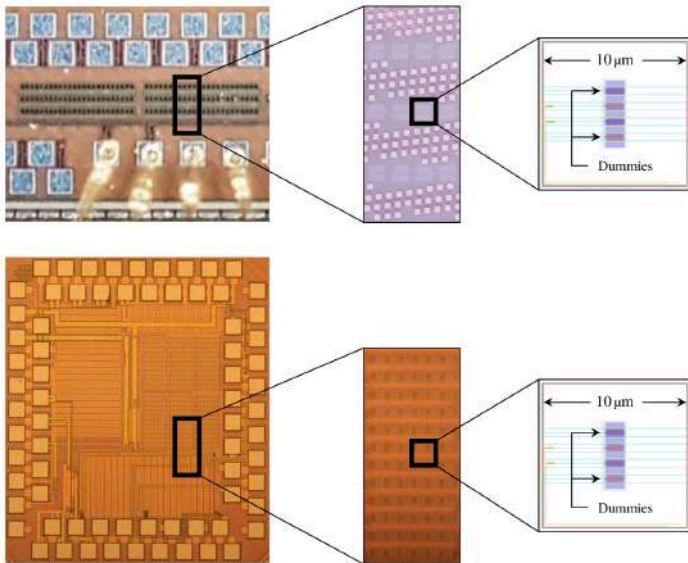


- Threshold voltage increases significantly
- A current kink may appear
- Mismatch in passives and actives is more prominent
- The substrate becomes practically floating
- *The SS is higher but it saturates around 1K*
- Leakage drastically reduces

R.M. Incandela et al., *ESSDERC* 2017

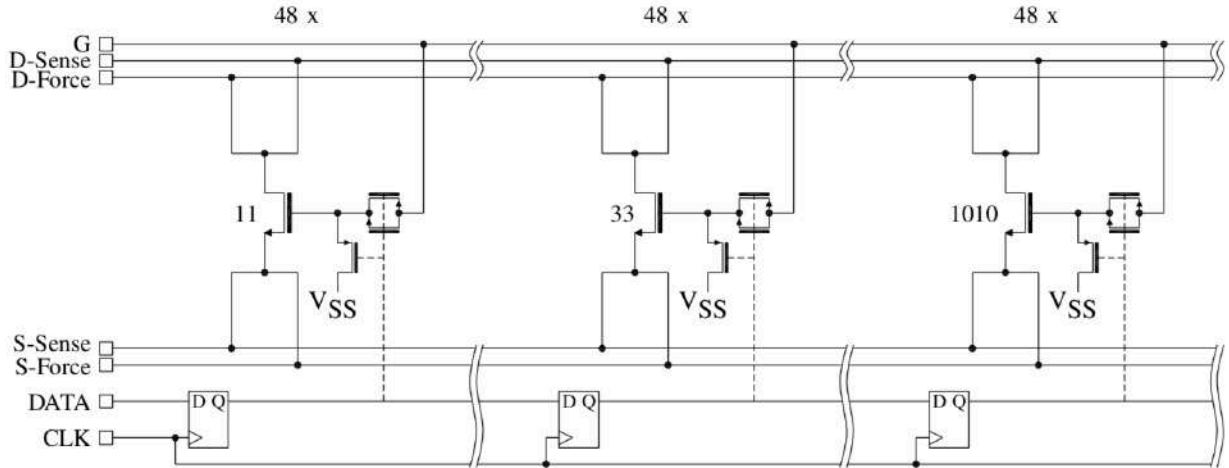
R.M. Incandela et al., *J. of EDS* 2018

How to Characterize MOS Transistors?



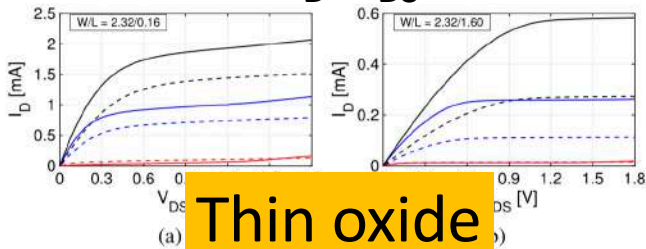
P. 't Hart et al., *J. EDS* 2020

CMOS Characterization in Practice

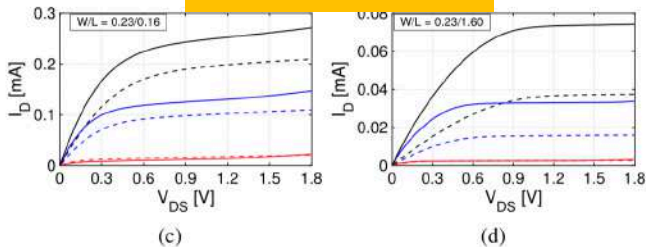


P. 't Hart et al., *J. EDS* 2020

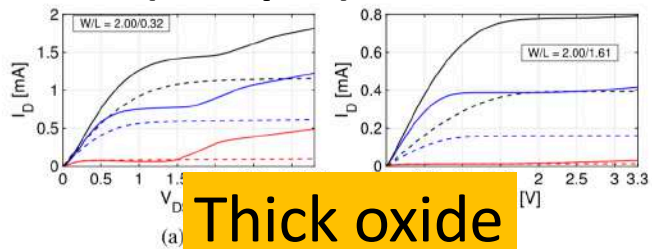
I_D - V_{DS} Characterization (0.16 μ m)



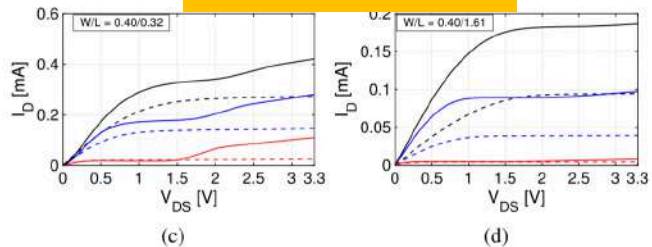
Thin oxide



$V_{GS} = [0.68 \text{ V}; 1.24 \text{ V}; 1.8 \text{ V}]$. Solid line: 4 K; dashed line: 300 K.

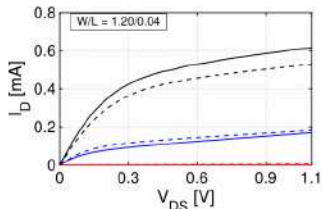


Thick oxide

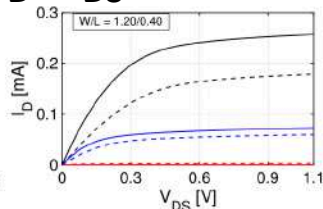


$V_{GS} = [1.05 \text{ V}; 2.17 \text{ V}; 3.3 \text{ V}]$. Solid line: 4 K; dashed line: 300 K.

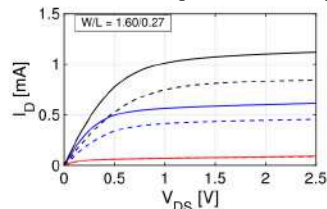
I_D - V_{DS} Characterization (40nm)



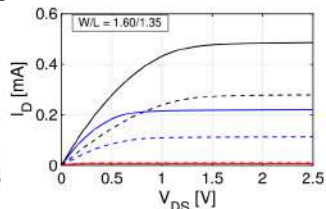
(a)



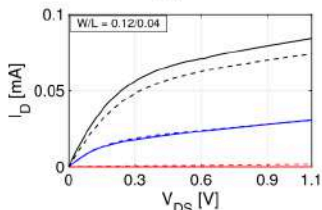
(b)



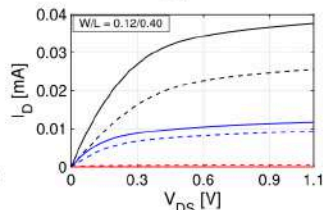
(a)



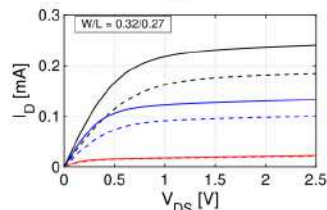
(b)



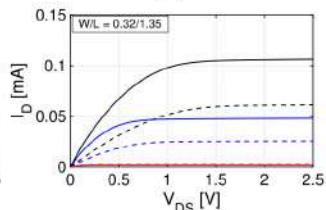
(c)



(d)



(c)

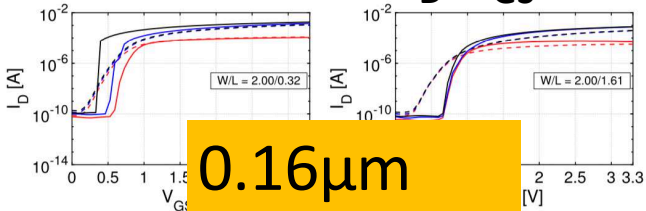


(d)

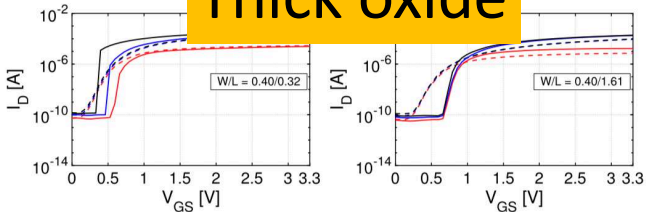
$V_{GS} = [0.43 \text{ V}; 0.76 \text{ V}; 1.1 \text{ V}]$. Solid line: 4 K; dashed line: 300 K.

$V_{GS} = [0.85 \text{ V}; 1.68 \text{ V}; 2.5 \text{ V}]$. Solid line: 4 K; dashed line: 300 K.

I_D - V_{GS} Characterization



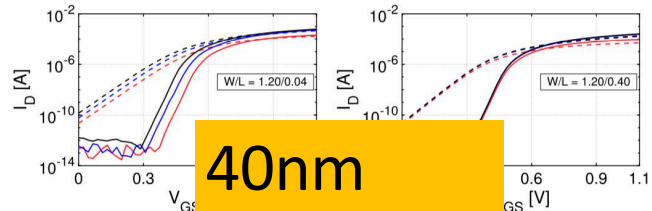
0.16 μ m
Thick oxide



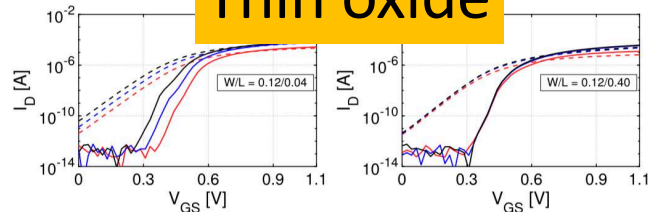
(c)

(d)

$V_{DS} = [0.1 \text{ V}; 1.7 \text{ V}; 3.3 \text{ V}]$. Solid line: 4 K; dashed line: 300 K.



40nm
Thin oxide

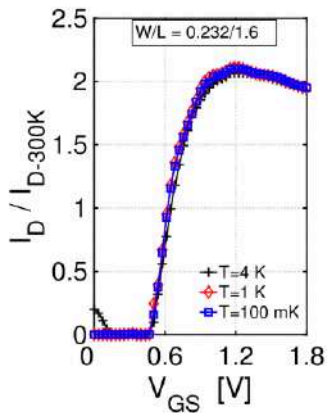


(c)

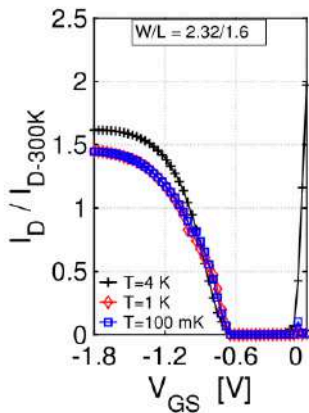
(d)

$V_{DS} = [0.1 \text{ V}; 0.6 \text{ V}; 1.1 \text{ V}]$. Solid line: 4 K; dashed line: 300 K.

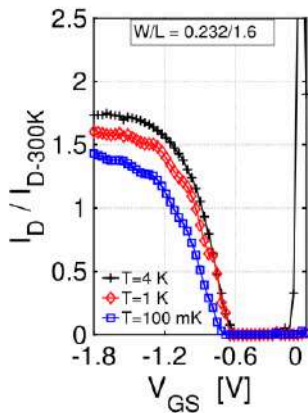
I_D - V_{GS} Characterization in Sub-K Regimes



NMOS
 $V_{DS} = 1.8V$



PMOS
 $V_{DS} = -1.8V$



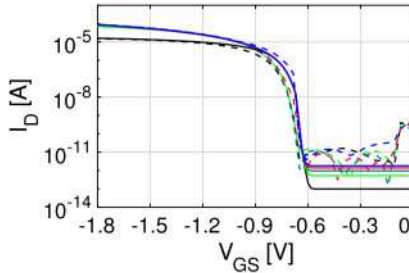
PMOS
 $V_{DS} = -1.8V$

R.M. Incandela et al., *J. of EDS* 2018

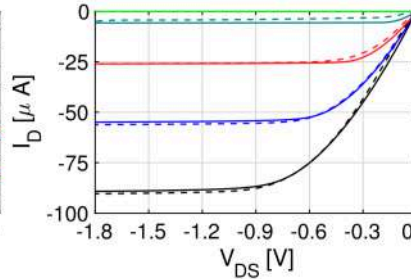
CMOS Modeling

MOS11 parameters for 0.16- μm CMOS					
BETSQR	VFBR	THESRR	SDIBLO	ALPR	KOR
THESATR	THERR	A1R	A2R	A3R	
PSP parameters for 40-nm CMOS					
FACTUO	DELVTO	THEMUO	THESATO	RSW1	CFL
ALPL	MUEO	FBET1			

Model ———
Measurement - - - -

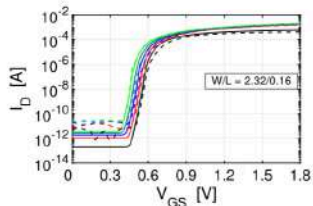


Thin oxide PMOS
 $V_{DS} = -1.8 - -0.09\text{V}$

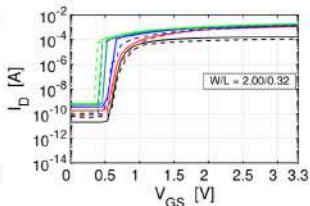


Thin oxide PMOS
 $V_{GS} = -1.3 - -1.8\text{V}$

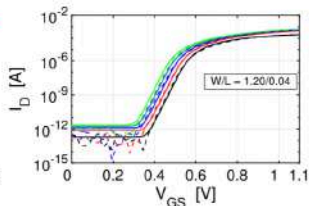
CMOS Modeling



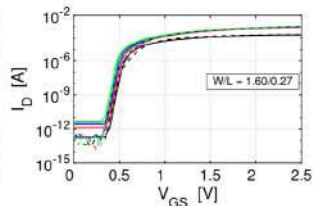
(a) 0.16 μm , thin oxide



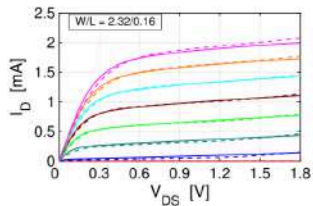
(b) 0.16 μm , thick oxide



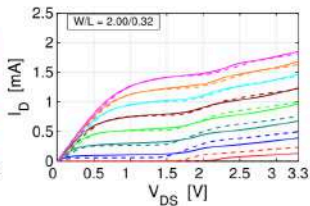
(c) 40 nm, thin oxide



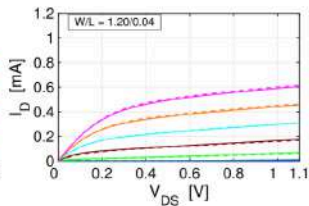
(d) 40 nm, thick oxide



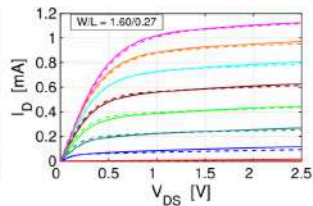
(e) 0.16 μm , thin oxide



(f) 0.16 μm , thick oxide



(g) 40 nm, thin oxide



(h) 40 nm, thick oxide

Sub-threshold Slope (SS)

$$SS = \ln(10) \frac{kT}{q} \left(1 + \frac{C_d}{C_{ox}}\right)$$

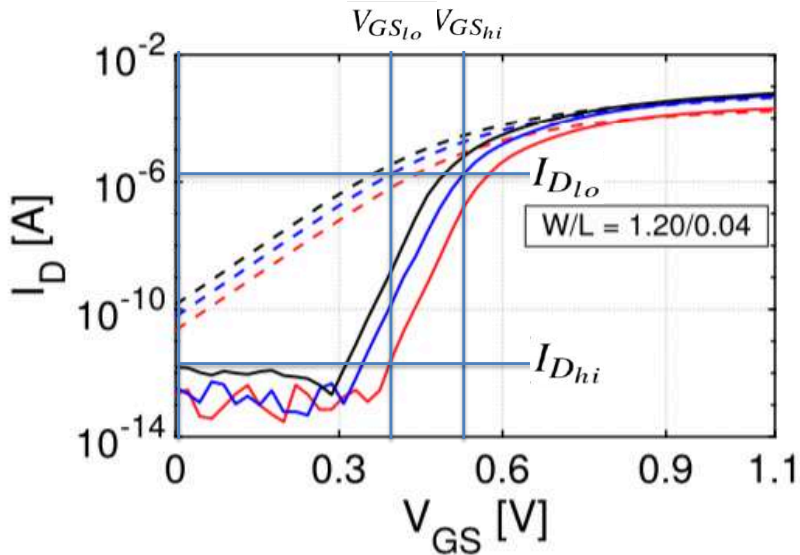
C_d = depletion layer capacitance

C_{ox} = gate oxide capacitance

$$SS = \ln(10) \frac{kT}{q} \sim 60\text{mV/dec}$$

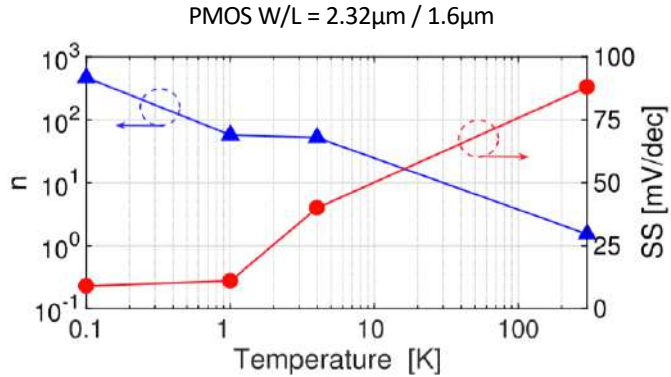
$C_d = 0$; $C_{ox} \rightarrow \infty$: thermionic limit

Sub-threshold Slope Characterization(SS)



$$SS^{-1} = \frac{|\log(I_{D_{hi}}/I_{D_{lo}})|}{V_{GS_{hi}} - V_{GS_{lo}}}$$

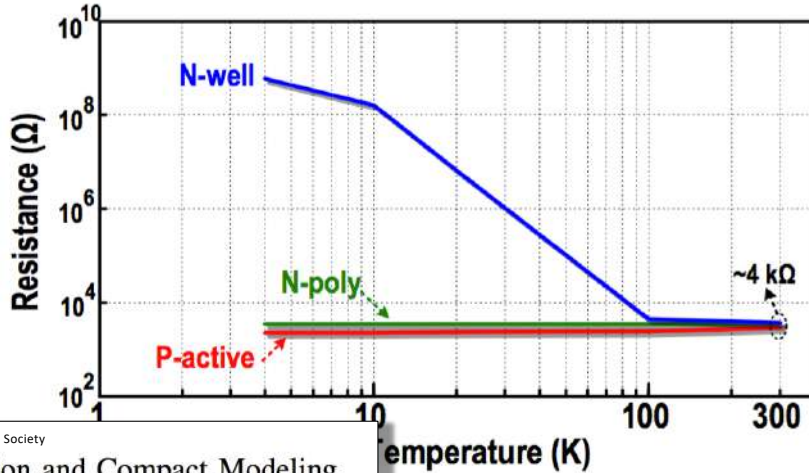
Sub-threshold Slope (SS)



R.M. Incandela et al., *ESSDERC* 2017

R.M. Incandela et al., *J. of EDS* 2018

Substrate Resistivity



IEEE Journal of the Electron Device Society

Characterization and Compact Modeling of Nanometer CMOS Transistors at Deep-Cryogenic Temperatures

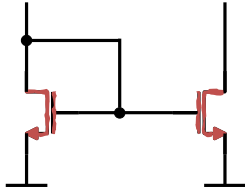
Rosario M. Incandela, *Student, IEEE*, Lin Song, Harald Hornulle, Edoardo Charbon, *Fellow, IEEE*,
Andrei Vladimirescu, *Fellow, IEEE*, and Fabio Sebastian, *Senior Member, IEEE*

ra et al., JSSC 2018

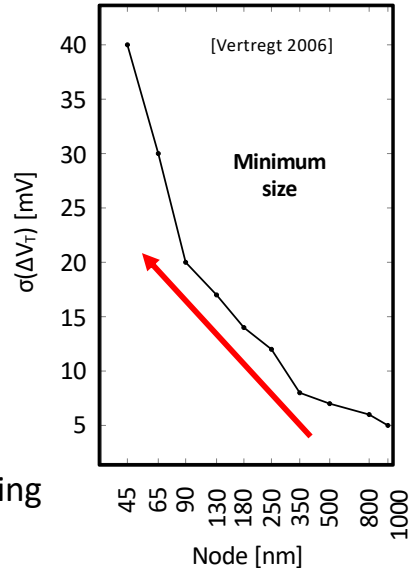
2021 Edoardo Charbon

Mismatch Modeling at Cryo

Subthreshold Current Mismatch: Why Do We Care?



- Impacts performance of:
 - ADC/DAC
 - Differential pairs
 - SRAM
- Worsens with technology scaling



Subthreshold Current Model

$$I_D = I_0 e^{(V_{GS} - V_{TH})/SS}$$

Taylor expansion is impractical at cryo due to the instability of I_D and the exponential nature of it.

Solve wrt $\log(I_D)$

$$\log(I_D) \propto \frac{1}{\ln(10)} \frac{V_{GS} - V_{TH}}{SS}.$$

Taylor expansion on V_{TH} and SS

$$\Delta \log(I_D) = \frac{1}{\ln(10)} \left(-\frac{1}{SS} \Delta V_{TH} - \frac{(V_{GS} - V_{TH})}{SS} \frac{\Delta SS}{SS} \right)$$

Subthreshold Current Model

$$\sigma_{\Delta \log I_D}^2 = \frac{1}{\ln(10)^2} \left[\left(\frac{\sigma_{\Delta V_{TH}}}{\overline{SS}} \right)^2 + \left(\frac{V_{GS} - V_{TH}}{\overline{SS}} \frac{\sigma_{\Delta SS}}{\overline{SS}} \right)^2 + 2 \frac{(V_{GS} - V_{TH})}{\overline{SS}^3} \sigma_{\Delta V_{TH}} \sigma_{\Delta SS} \rho_{\Delta V_{TH}, \Delta SS} \right]. \quad (5)$$

The correlation factor ρ between V_{TH} and SS is generally negligible at 300K, 100K, and also at cryogenic temperatures.

Croon Model

$$\sigma_{\Delta I_D / I_D}^2 = \ln(10)^2 \sigma_{\Delta \log I_D}^2$$

$$\sigma_{\Delta \log I_D}^2 = \frac{1}{\ln(10)^2} \left[\sigma_{\Delta \beta / \beta}^2 + \left(\frac{\bar{g}_m}{\bar{I}_D} \right)^2 \sigma_{\Delta V_{TH}}^2 \right], \quad (7)$$

Pelgrom Scaling Law

$$\sigma_{\Delta V_{TH}} = \frac{A_{VT}}{\sqrt{WL}} \quad \sigma_{\Delta\beta/\beta} = \frac{A_{\beta}}{\sqrt{WL}} \quad \sigma_{\Delta SS/SS} = \frac{A_{SS}}{\sqrt{WL}}$$

A_{VT} : area scaling parameter for V_T

A_{β} : area scaling parameter for β

A_{SS} : area scaling parameter for SS

W, L : transistor geometry parameters

How to Characterize Mismatch?

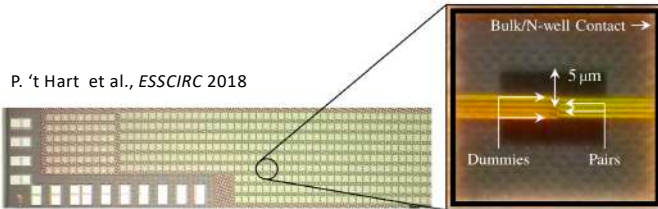
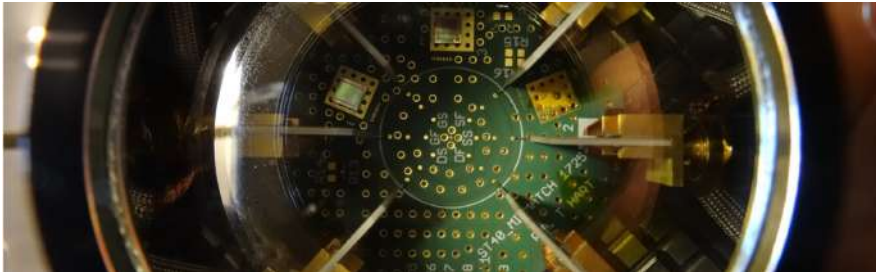
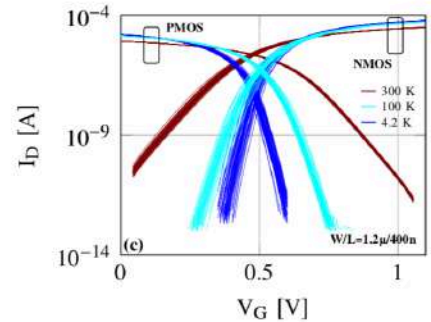
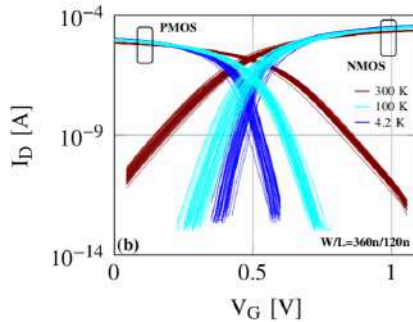
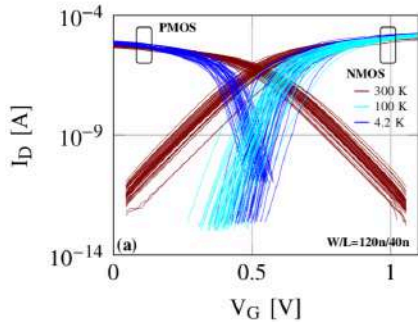


Fig. 1. Die micrograph (*left*) with close-up of a $W/L = 1.2\text{ }\mu\text{m}/0.4\text{ }\mu\text{m}$ matched pair (*right*).

Mismatch Measurements



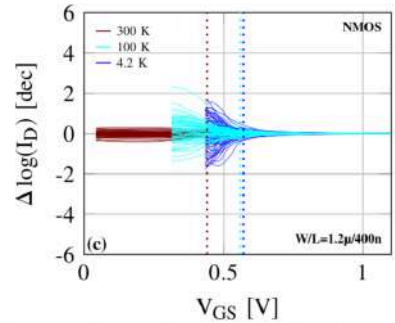
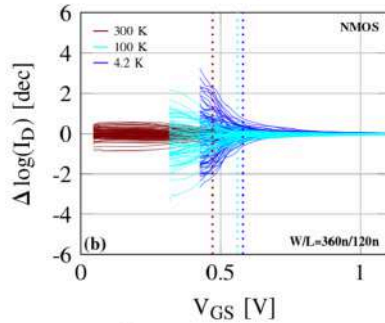
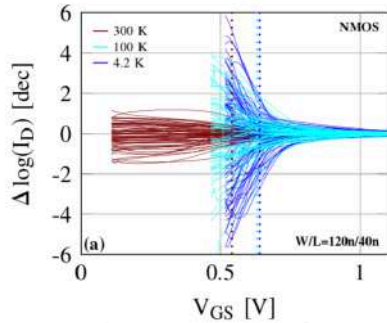
48 devices tested

$|V_{DS}| = 50\text{mV}$, $V_S = 0\text{V}$ (NMOS)

$|V_{DS}| = 50\text{mV}$, $V_S = 1.1\text{V}$ (PMOS)

P. 't Hart et al., *J. of EDS* 2020

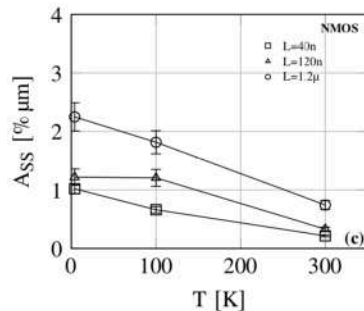
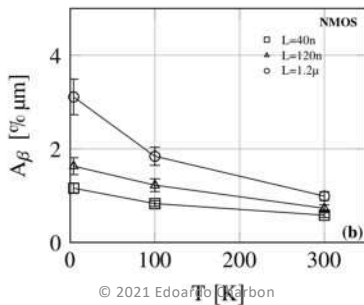
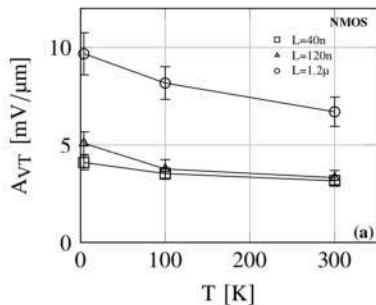
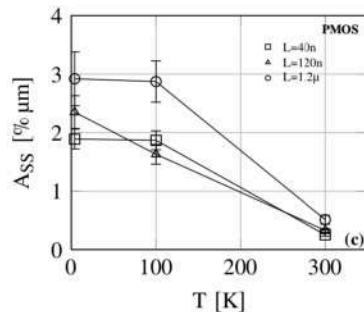
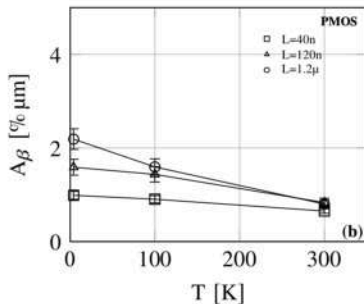
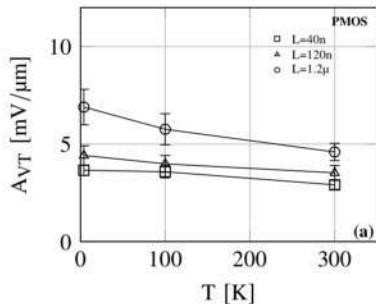
Mismatch Measurements (2)



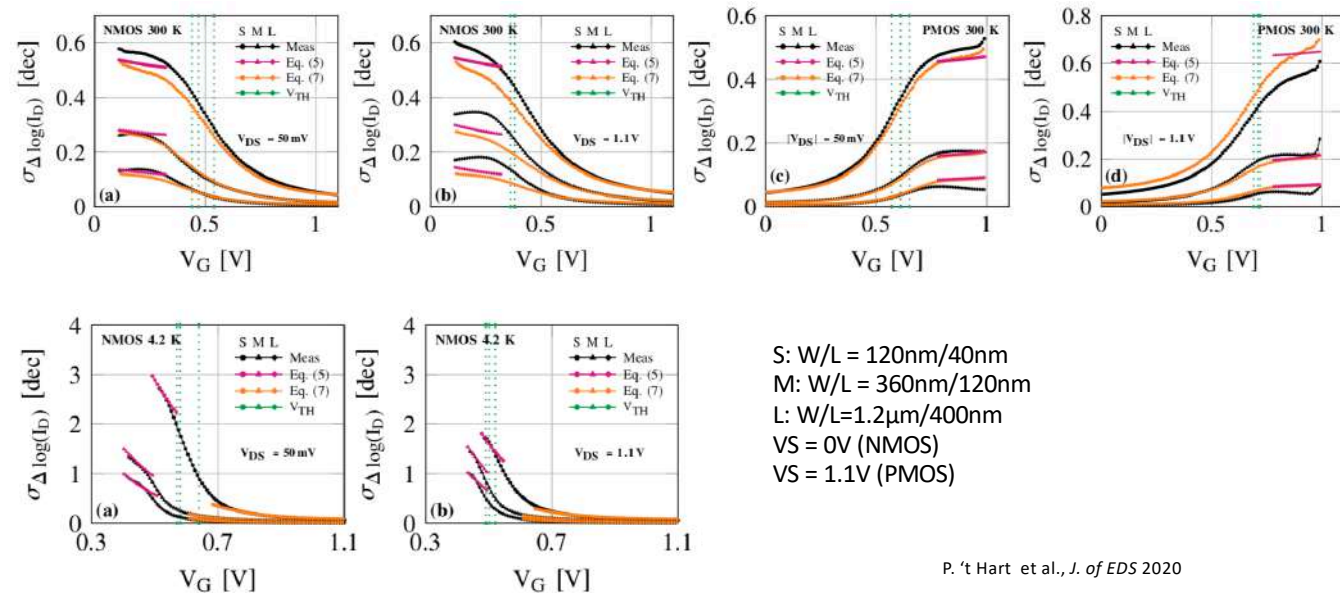
72 device pairs tested
 V_{TH} in dashed lines
 $|V_{DS}| = 50mV$

P. 't Hart et al., *J. of EDS* 2020

Pelgrom Area Scaling Parameters



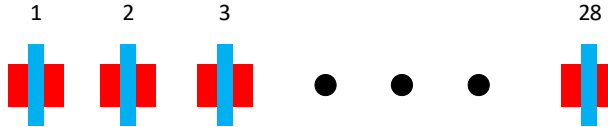
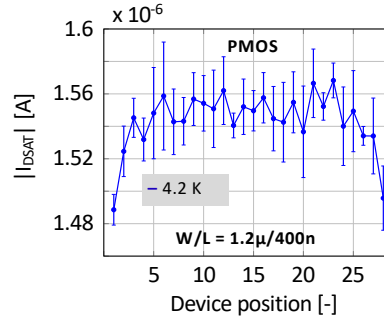
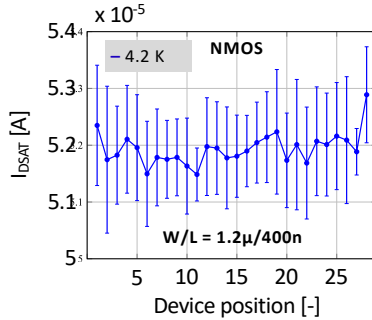
Mismatch Modeling



S: W/L = 120nm/40nm
M: W/L = 360nm/120nm
L: W/L = 1.2 μ m/400nm
VS = 0V (NMOS)
VS = 1.1V (PMOS)

P. 't Hart et al., *J. of EDS* 2020

Position Dependence



Summary on Threshold Mismatch

- Cryo-CMOS: mismatch follows Pelgrom and Croon models
- Fixed V_{GS} biasing \rightarrow matching deteriorates up to 10x
- Fixed G_m/I_D biasing \rightarrow matching deteriorates “only” 1.1x

Digital Modeling at Cryo

Lowerbound in Digital Design

$$V_{DD,min} \approx 2 \frac{kT}{q} \ln(2) = 36\text{mV}$$

CMOS circuits operate in subthreshold wherever this equation holds

$$I_{DS} = I_0 \frac{W}{L} e^{\frac{V_{GS}-V_{TH}}{nv_t}} \left(1 - e^{-\frac{V_{DS}}{v_t}}\right); I_0 = \mu_0 C_{ox} \frac{W}{L} (n-1)v_t^2,$$

n is the sub-threshold slope (SS) factor and $v_t = kT/q$,

The net effect in sub-threshold regimes is a decrease of leakage currents by orders of magnitude, implying a significant increase in the I_{ON}/I_{OFF} ratio

Lowerbound in Digital Design

Assuming an ideal SS factor $n = 1$, at 4.2 K, according to well established room temperature models, one could theoretically achieve $V_{DD,min} \approx 2 \ln(2)v_t = 0.48\text{mV}$.

However, at 4.2 K the consensus is that $n \approx 34.9$. Thus, this fundamental limit is actually $V_{DD,min} \approx 2.47\text{mV}$. Additional non-idealities include reverse short-channel effect (RSCE) and inverse narrow-width effect (INWE).

Both effects substantially modulate the threshold voltage.

Latchup

Latch-up has been found to be unpredictable in deep-cryogenic operation. Latch-up immunity typically improves at temperatures lower than RT, thanks to lower well and substrate resistance and to higher base-emitter voltages and lower current gain of parasitic bipolar transistors. However, shallow level impact ionization (SLII), a mechanism for carrier generation, emerges below 50 K

Recommendations

- A) create extensive substrate contacts and well-taps, so as to minimize the chance of latch-up at 4.2 K;
- B) resize the transistors, so as to reduce INWE and thus maximize V_{TH} modulation;
- C) add secondary power rails to enable forward back-biasing, so as to compensate for an increase of V_{TH} at 4.2, in addition use low- V_{TH} transistors;
- D) minimize the length of transistors (in contrast to conventional RT sub-threshold standard cell design, where the opposite is generally done);
- E) when useful, make the layout aware of mismatch by increasing the overall height of the cells.

Summary of Issues 300K → 0.1K

- Threshold voltage increases significantly
- A current kink may appear
- Mismatch in passives and actives is more prominent
- The substrate becomes practically floating
- The SS is higher but it saturates around 1K
- Leakage drastically reduces

Trends and Predictions

- How will devices perform in 5 years at 77K?
- How will FinFETs/nanowire FET behave at 77K ($L_g < 20\text{nm}$)
- Will ballistic transport affect these devices?
- How different will optimization be at 77K?
- Is there a way to decrease V_T ?

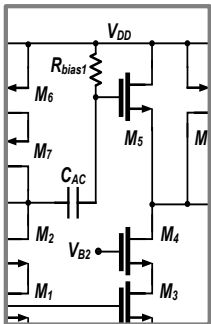
High-Level Modeling at Cryo

High-Level Modeling: SPINE (SPIN Emulator)

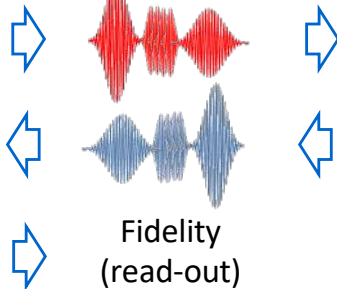
Objectives:

- Enable co-design qubit/electronics
- Derive specifications for Horse Ridge and other components
- Minimize power to achieve wanted fidelity

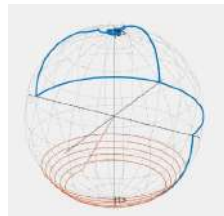
Circuit simulator



Electrical signals

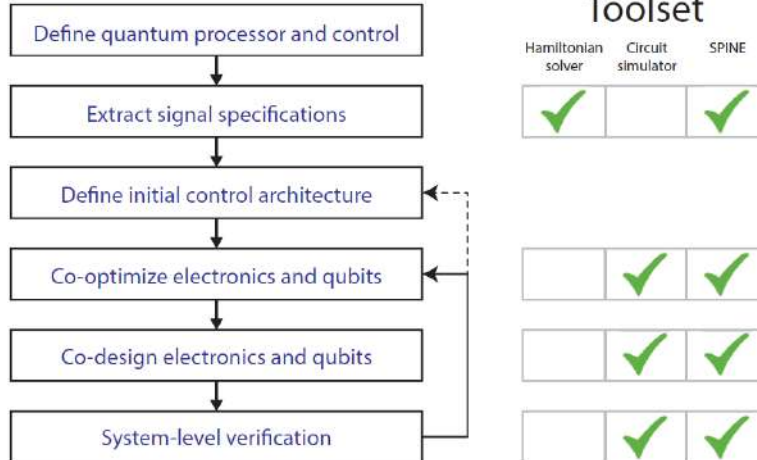


Qubit simulator
(Hamiltonian)



Fidelity

SPINE

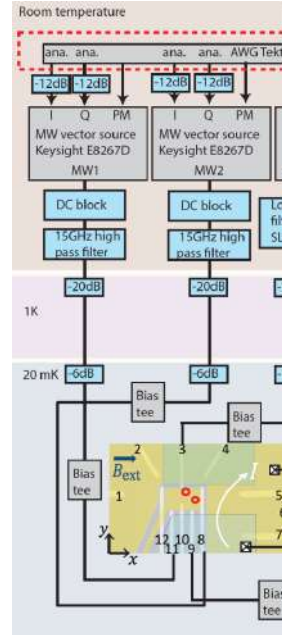


J. Van Dijk *et al.*, DATE 2018

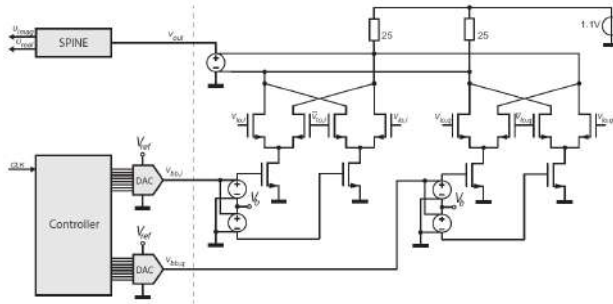
SPINE

- Microwave Carrier: **Keysight E8267D**
 - 22.4 kHz resolution 1 mHz
 - $\mathcal{L}(1 \text{ MHz}) = -106 \text{ dBc/Hz}$ >15 dB better
 - $S_n = 7.12 \text{ nV/VHz}$ 63 nV/VHz
→ > 20 dB attenuation
- Microwave Envelope: **Tektronix 5014C**
 - 8-bit resolution 14-bit
 - 140 MS/s 1.2 GS/s
 - $3.56 \text{ ns}_{\text{rms}}$ 5.0 ps_{rms}
 - 40 dB SNR better

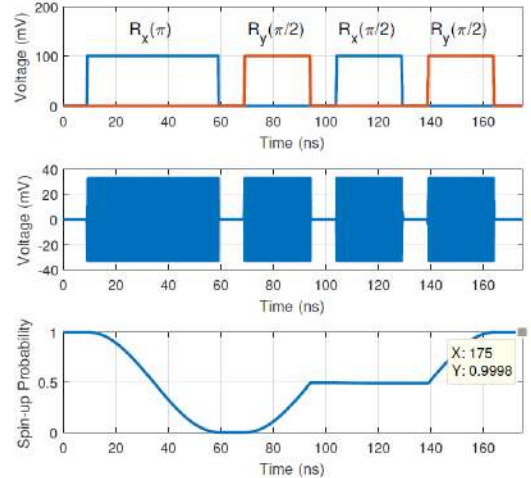
With SPINE we checked that these specs are enough



SPINE



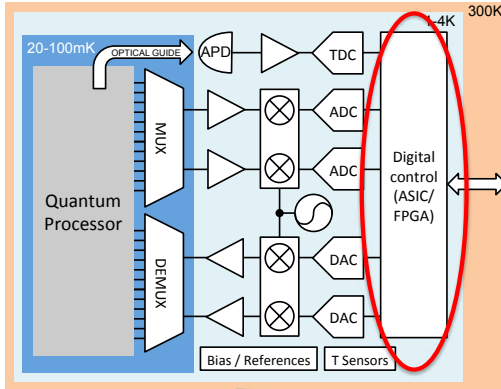
- Example of full simulation:
 - Sequence of rotations
 - Resulting RF signals
 - Qubit response, in terms of spin-up probability
- This involves spin emulation, M/S simulation, RF simulation



J. Van Dijk *et al.*, DATE 2018

Cryogenic Reconfigurable Hardware

Cryo-FPGAs



Cryo-FPGAs

CryoCMOS Hardware Technology A Classical Infrastructure for a Scalable Quantum Computer

ACM Frontiers in Computing, Como 2016

Harald Homulle¹, Stefan Visser¹, Bishnu Patra¹, Giorgio Ferrari², Enrico Prati³,
Carmen G. Almudéver¹, Koen Bertels¹, Fabio Sebastiano¹, Edoardo Charbon¹

¹QuTech, Delft University of Technology, Delft, The Netherlands

²Politecnico di Milano, Milano, Italy, ³Consiglio Nazionale delle Ricerche, Milano, Italy
{h.a.r.homulle, f.sebastiano, e.charbon@tudelft.nl}



FPGA functionality

- All FPGA components are working in the cryogenic environment down to 4K
- No modifications required

Component	Functional	Behavior
IOs	✓	
LVDS	✓	
LUTs	✓	Delay change < 5%
CARRY4	✓	Delay change < 2%
BRAM	✓	No corruption (800 kB)
MMCM	✓	Jitter reduction of roughly 20%
PLL	✓	Jitter reduction of roughly 20%
IDELAYE2	✓	Delay change of up to 30%
DSP48E1	✓	No corruption over 400 operations

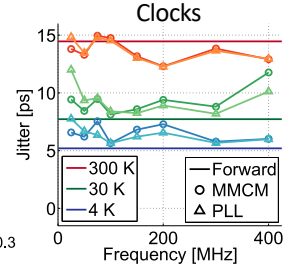
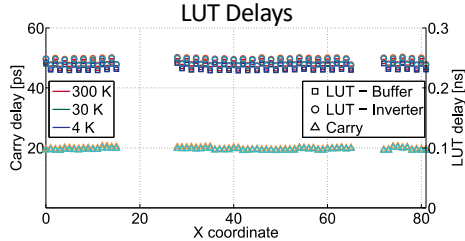
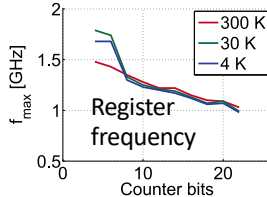
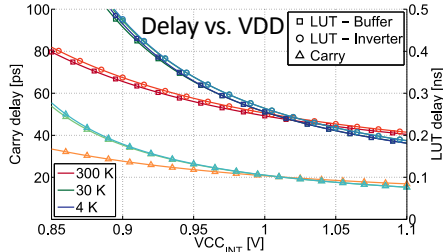
FPGA Performance

Specs:

Carry: 20 vs. 8.4 ps at 300 K

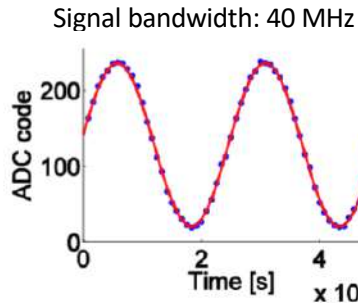
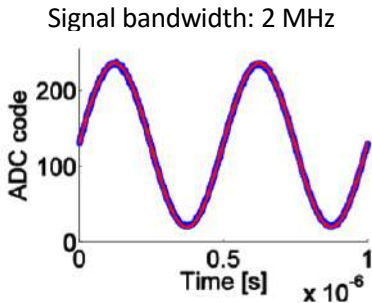
LUTs: 238 vs 235 ps at 300 K

Speed-up 2.4 vs 10.8% toward 300 K

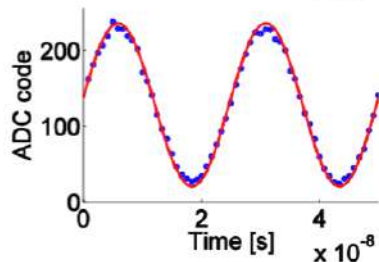
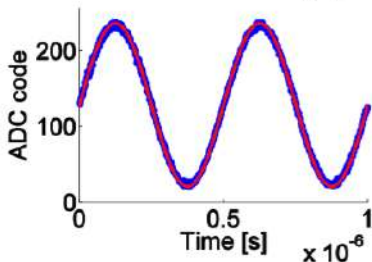


ADC on FPGA (1.2GSa/s)

300K



15K



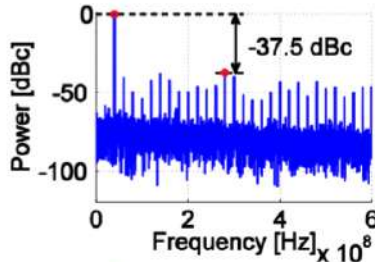
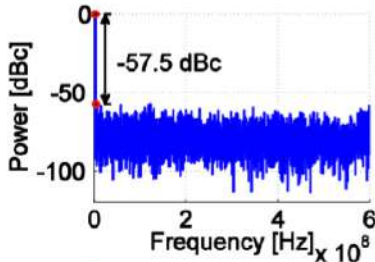
H. Homulle et al., TCAS I, 63(11), 1854-1865, 2016

ADC on FPGA

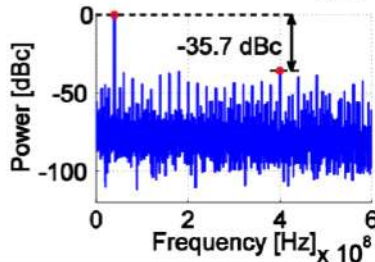
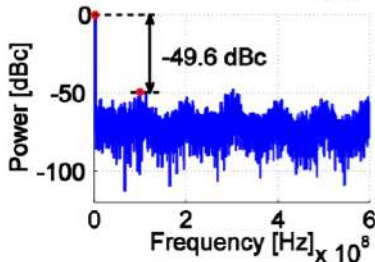
Signal bandwidth: 2 MHz

Signal bandwidth: 40 MHz

300K



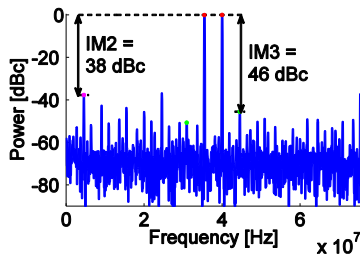
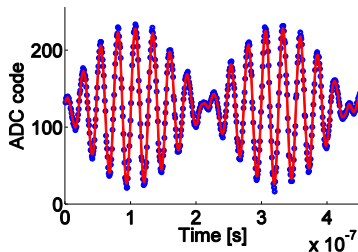
15K



H. Homulle et al., TCAS I, 63(11), 1854-1865, 2016

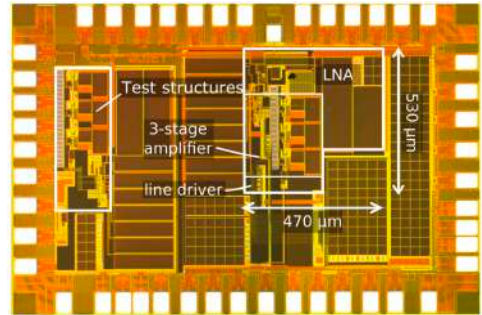
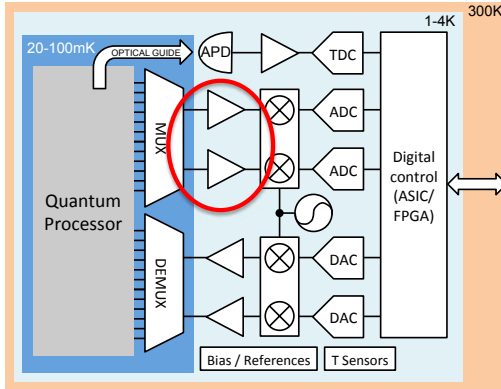
Distortion (IM2, IM3)

- Two tones: $\approx 36 / 41$ MHz
 - IM2 = 38 dB
 - IM3 = 46 dB
- Many secondary harmonics
- Interference with 100 MHz (sampling tone)

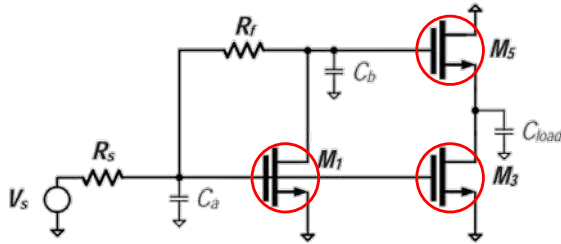


Cryogenic ASICs

Low Noise Amplifiers (Cryo-LNAs)

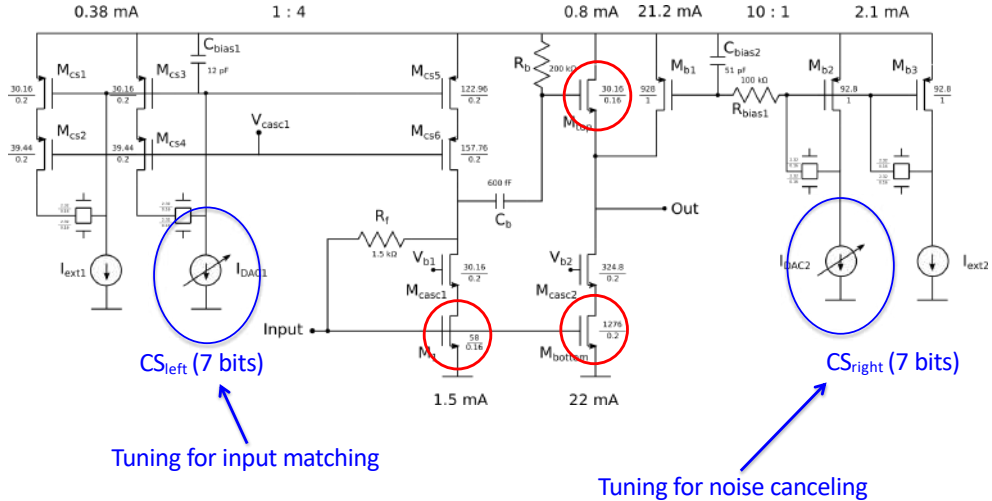


Cryo-LNA

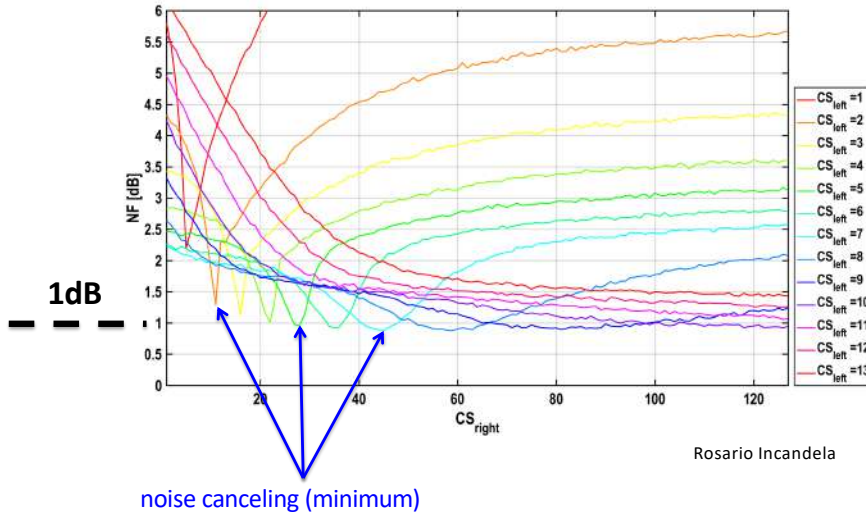
F. Bruccoleri et al., *JSSC* 2004

- Standard 160nm CMOS
- 500 MHz Bandwidth
- 0.1dB Noise figure
- 7K noise-equivalent temperature

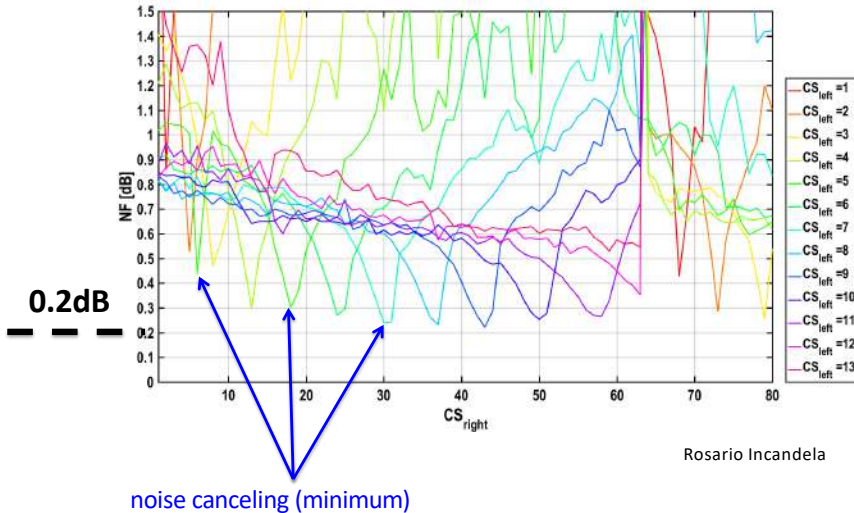
Cryo-LNA



Noise Figure at RT

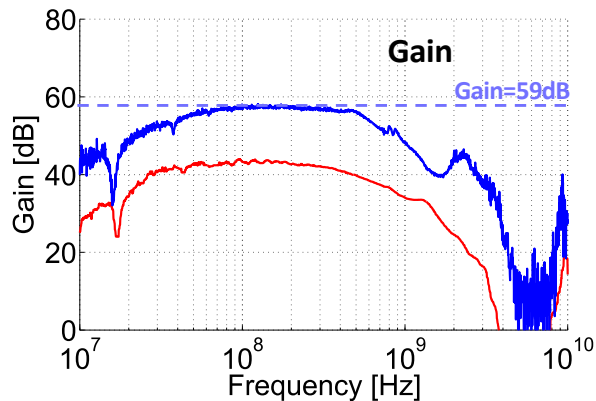


Noise Figure at 4K

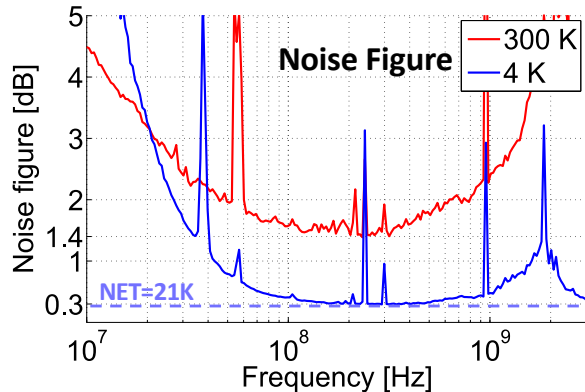


Rosario Incandela

Gain and Noise

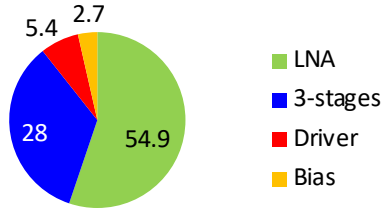


B. Patra, R. Incandela et al, *JSSC* 2018



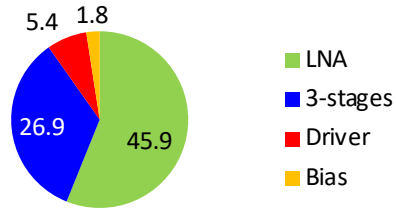
Power

Power consumption at 4 K [mW]



Measured: **91mW**

Power consumption at 300 K [mW]



Measured: **80mW**

Sharing 150x 1MHz-channels (one channel per qubit)


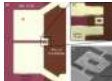
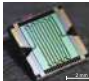
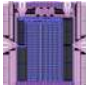
=

0.61mW per qubit

Rosario Incandela



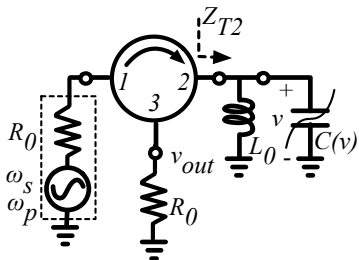
Can We Do Better?

Amplifier Metrics	Cryogenic HEMT	JPA	TWPA 1.0	TWPA 2.0
				
Power Dissipation	16 mW	100 pW	1 nW	5 nW
Bandwidth (>15 dB gain)	11 GHz	100 - 200 MHz	6 GHz	5 GHz
1-dB Compression point	0 dBm	-110 dBm (3 qubits)	-95 dBm (20-30 qubits)	-85 dBm (> 100 qubits)
Noise Temperature	5 K	400 mK	400 mK	400 mK
External Hardware	Isolator	Direct. Coupler, Circulator	Direct. Coupler	None

Courtesy: David Hover and Greg Calusine, MIT Lincoln Laboratory

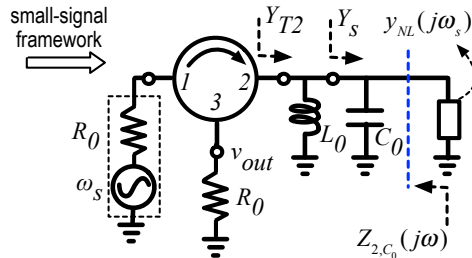
© 2021 Edoardo Charbon

Can We Do Better?

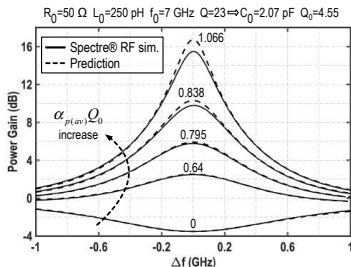


$$y_{NL}(j\omega_s) \approx -\omega_s \omega_i (\alpha_p C_0)^2 Z_{2,C_0}^*(j\omega_i)$$

$$\alpha_p \equiv K_1 V_p$$



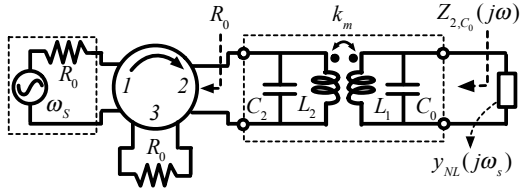
$$G_{T_{\max}}|_{Q \rightarrow \infty} = \left| \frac{1 + (\alpha_p Q_0)^2}{1 - (\alpha_p Q_0)^2} \right|^2$$



Major challenges:

- Narrowband
- Phase sensitive
- Large pump signal
- T_n limit of 4K @ 4K

CMOS Parametric Amplifier

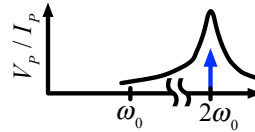


1) Transformer-based parametric amplifier

- ✓ Allow for broadband operation

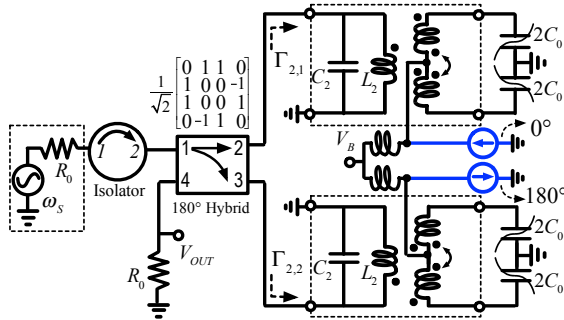
2) CM impedance peaking

- ✓ Suppress the pump signal leak
- ✓ Reduce pump power consumption

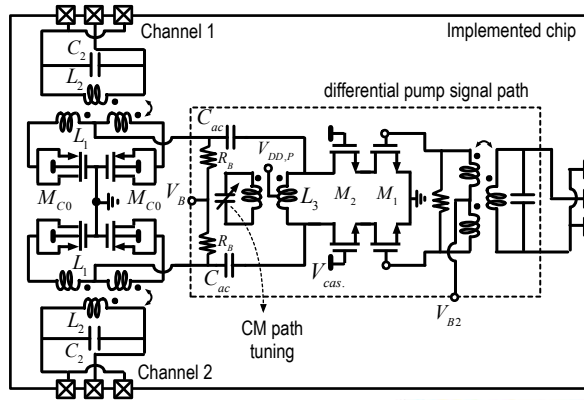


3) “image”-rejection architecture

- ✓ Double the usable RF bandwidth
- ✓ Phase-insensitive operation
- ✓ Allow for T_n limit of below 4K

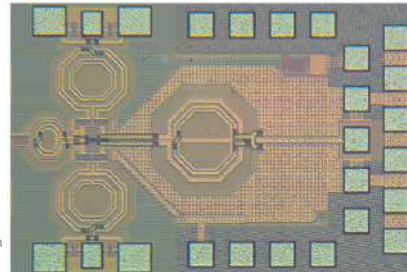
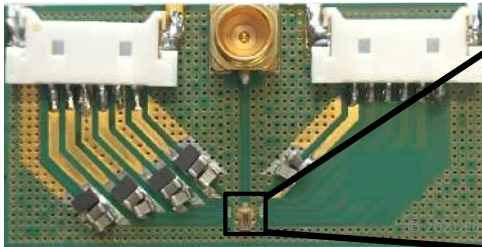


CMOS PA Architecture

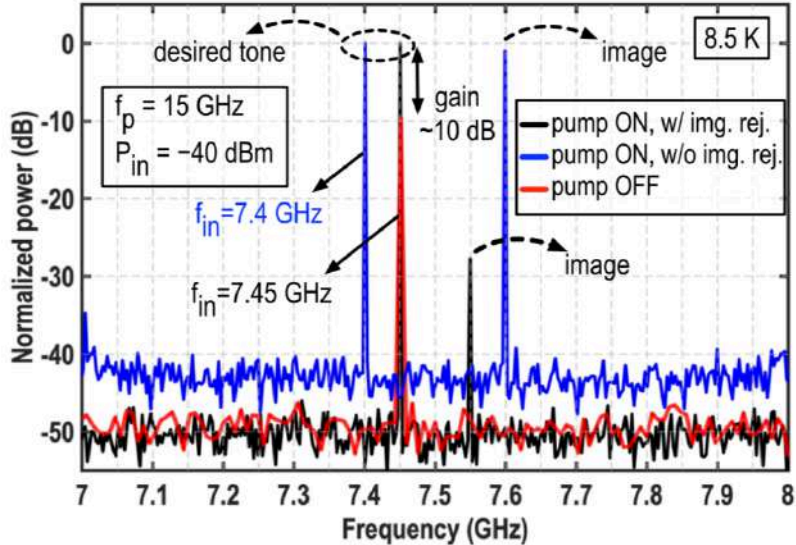


M. Mehrpoo, F. Sebastiano, E. Charbon, M. Babaie, *Solid-State Circuit Letters*, 2020

0.825 mm²

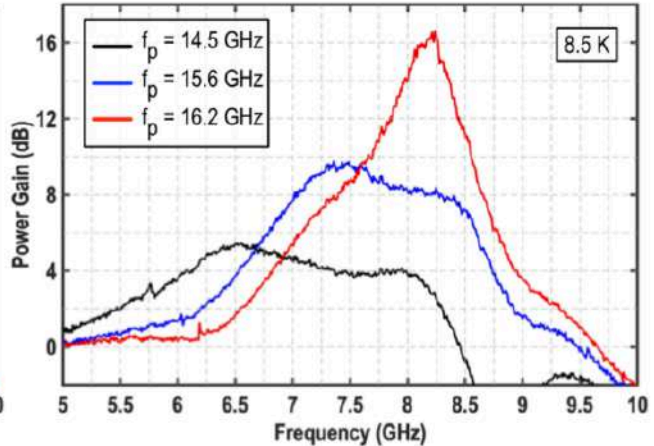
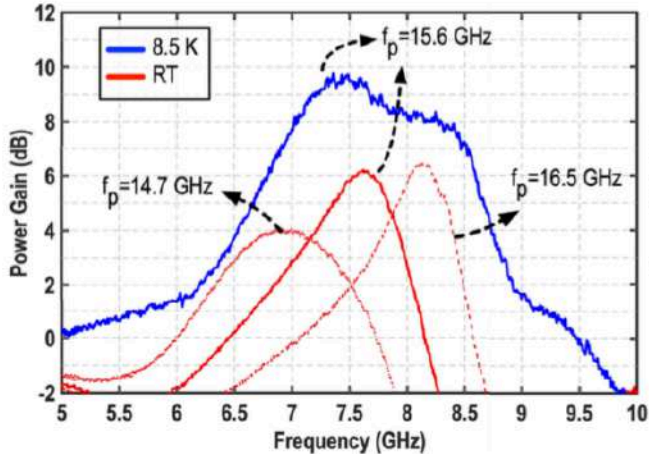


Spectrum of Single Tone



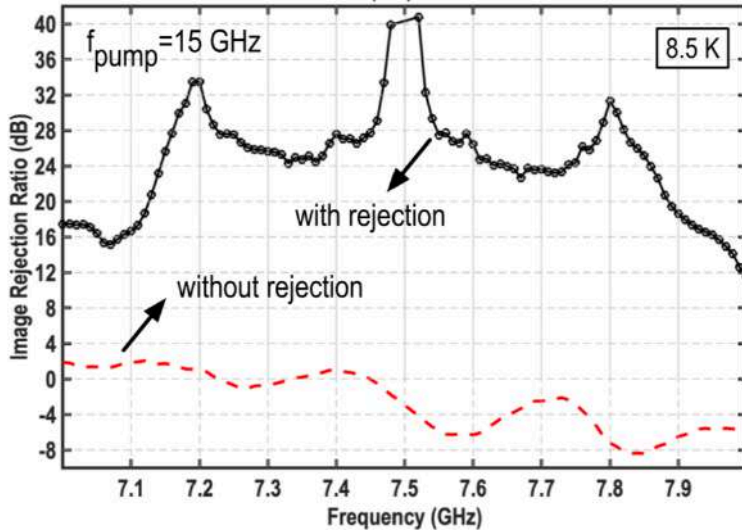
M. Mehrpoo, F. Sebastiano, E. Charbon, M. Babaie, *Solid-State Circuit Letters*, 2020

Power Gain vs. Pump Frequency and Temperature



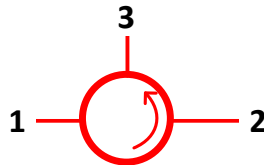
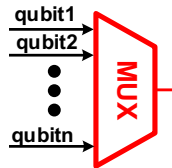
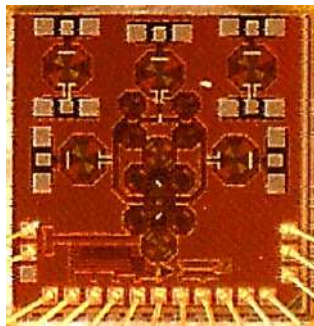
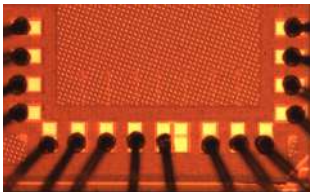
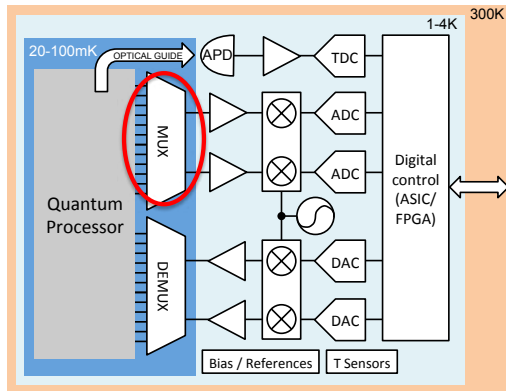
M. Mehrpoo, F. Sebastiano, E. Charbon, M. Babaie, *Solid-State Circuit Letters*, 2020

Image Rejection

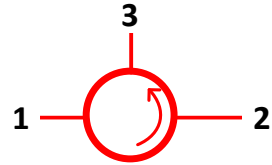
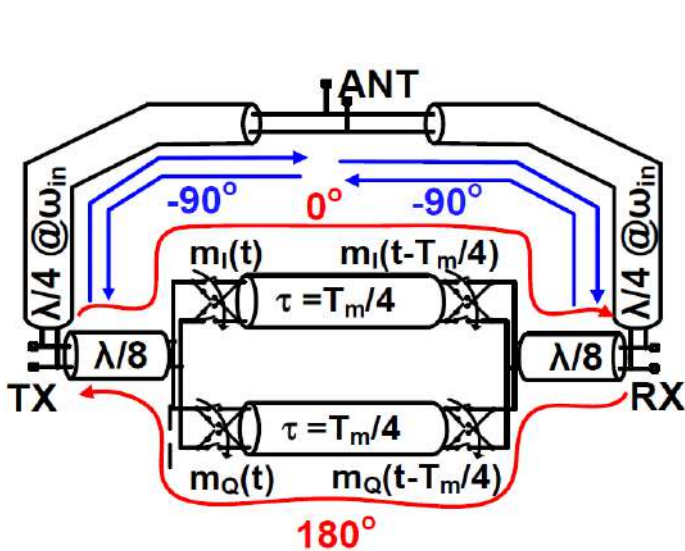


M. Mehrpoo, F. Sebastiano, E. Charbon, M. Babaie, *Solid-State Circuit Letters*, 2020

CMOS Passive Circulators & Multiplexers



Transmission Line Circulator



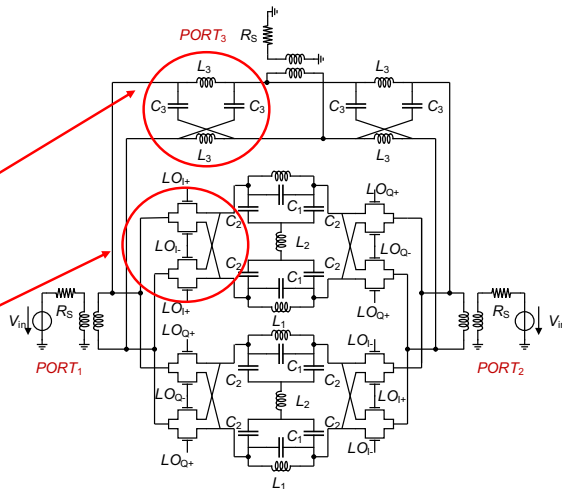
S-parameters

at $\omega_{in} = 3\omega_m$

$$S = \begin{bmatrix} 0 & 0 & -1 \\ -j & 0 & 0 \\ 0 & -j & 0 \end{bmatrix}$$

Passive Circulator Architecture

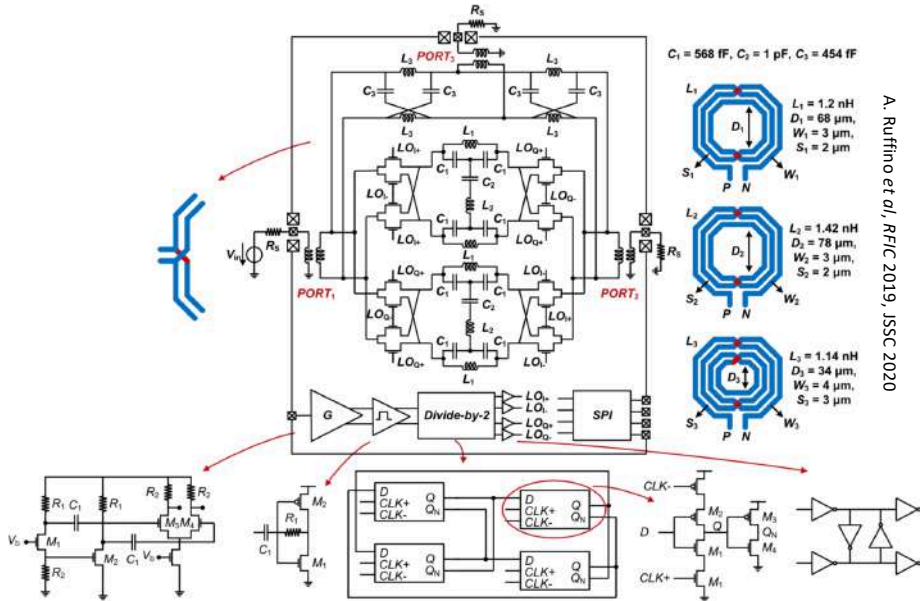
- Non-reciprocal behavior due to staggered commutation
- Passive LC all-pass filters
- Passive mixers with non-overlapping I/Q phases
- On-chip LO divider and I/Q generation
- SPI control for tunability



$$P_{DC} = 1.7 \text{ mW}$$

$$P_{AUX} = 8 \text{ mW}$$

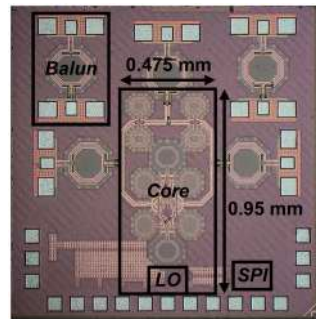
Passive Circulator Architecture



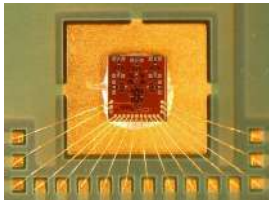
A. Ruffino et al, RFIC 2019, JSSC 2020

CMOS 40 nm Circulator Prototype

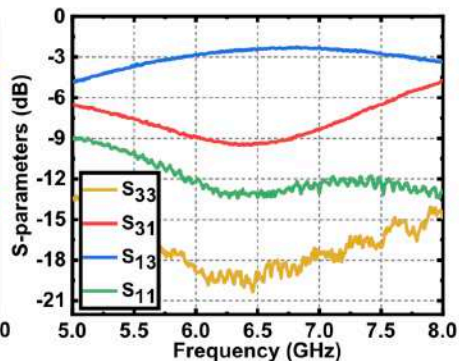
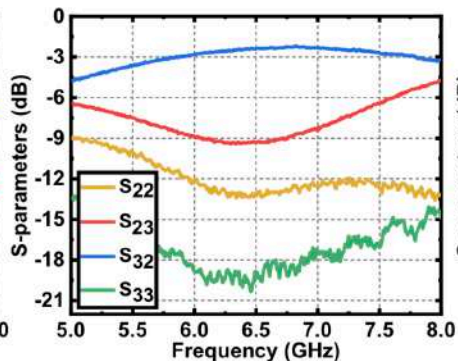
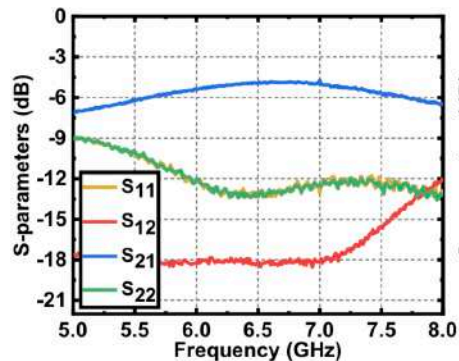
- TSMC CMOS 40 nm technology
- Tape-out, PCB design and measurements at 300 K and 4.2 K
- RF probing with LakeShore CPX probe station



A. Ruffino *et al*, *RFIC* 2019, *JSSC* 2020

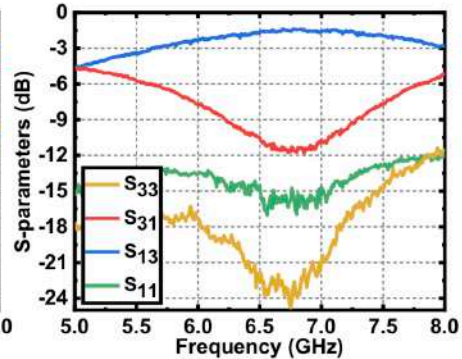
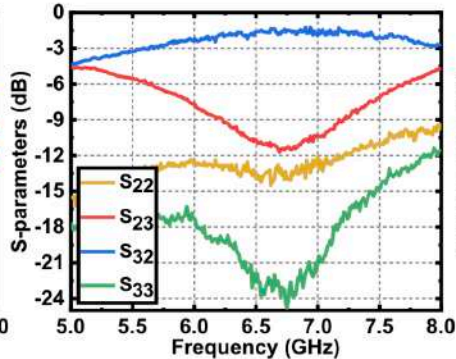
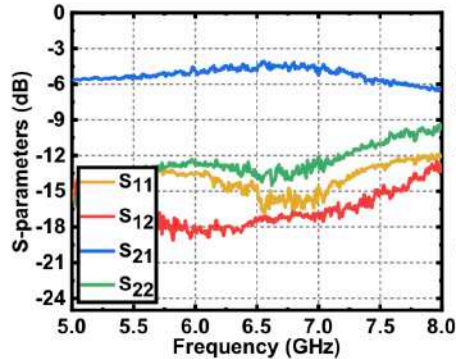


Measured S-parameters (300K)



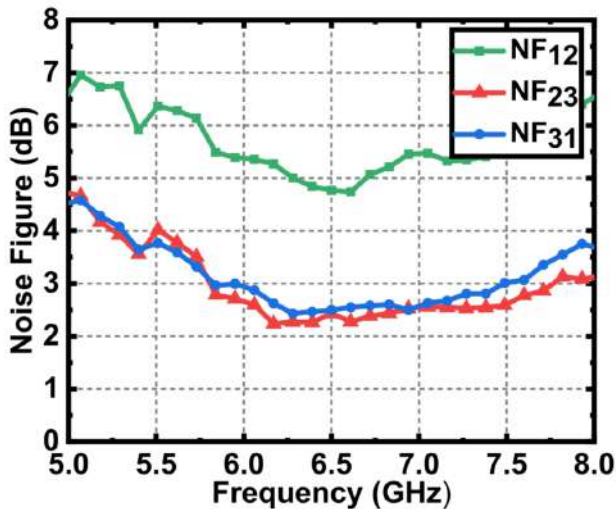
A. Ruffino et al, RFIC 2019, JSSC 2020

Measured S-parameters (4.2K)



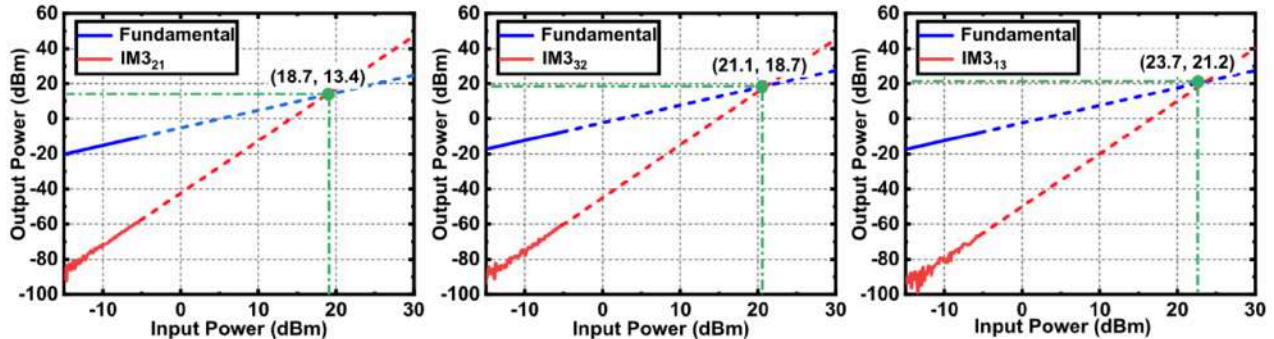
A. Ruffino et al, RFIC 2019, JSSC 2020

Circulator Noise Figure (300K)



Minimum noise figure of 2.1 dB is measured, consistent with insertion loss measurements. There is no excess noise from clock generation path.

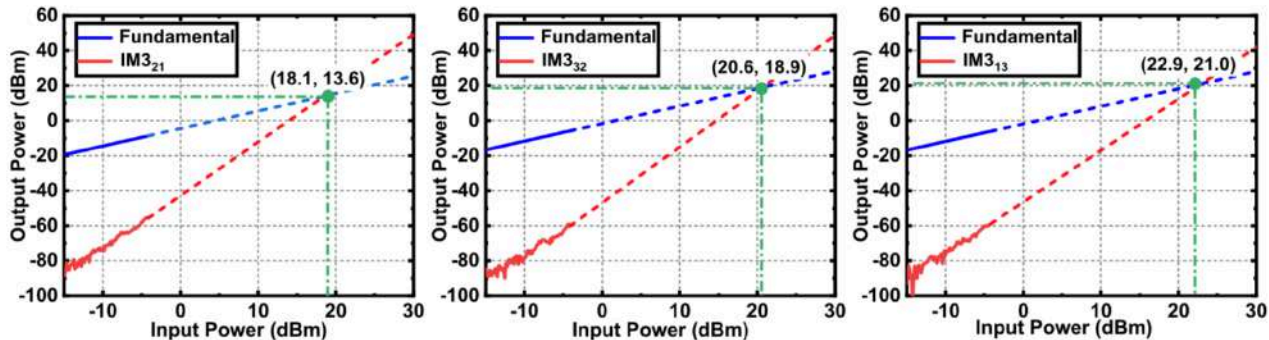
Circulator Linearity (300K)



A. Ruffino *et al*, *RFIC* 2019, *JSSC* 2020

High linearity is measured in all directions, due to the quasi-passive nature of the circulator.

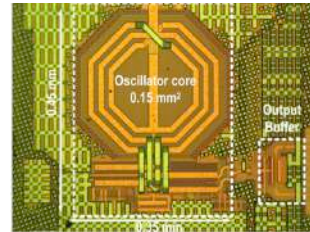
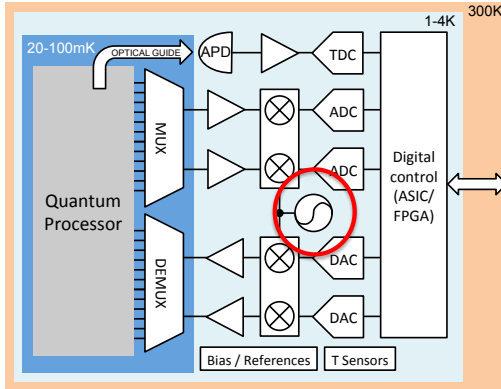
Circulator Linearity (4.2K)



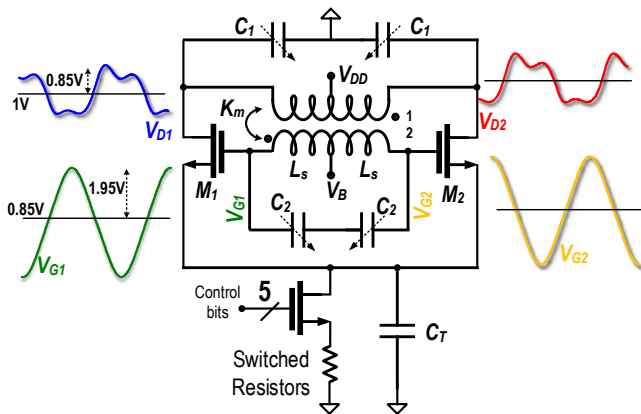
A. Ruffino et al, *RFIC* 2019, *JSSC* 2020

High linearity is measured in all directions, due to the quasi-passive nature of the circulator.

Cryo-Oscillators

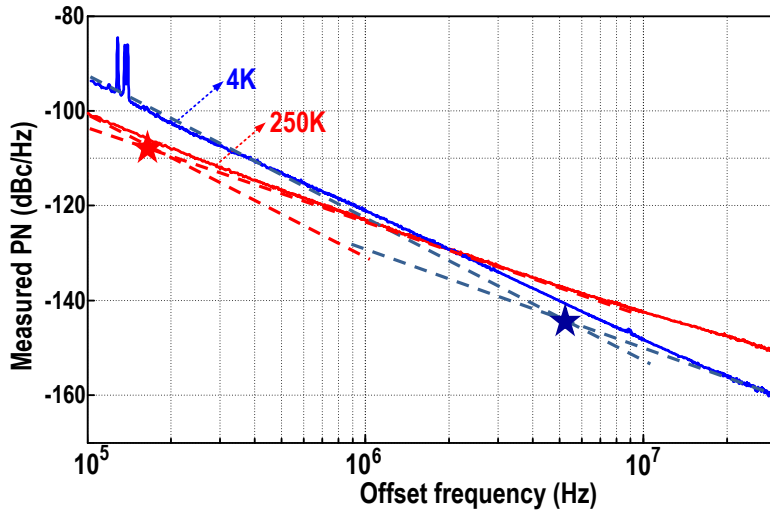


Cryo-Oscillator (Class F)

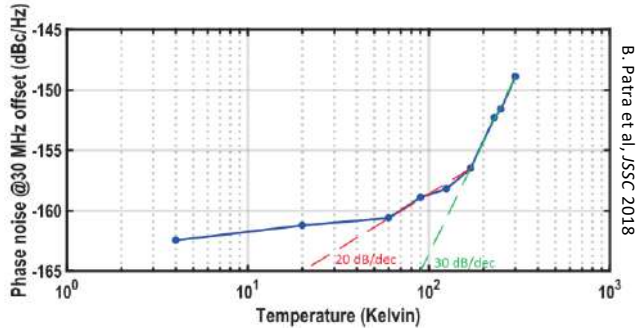


M. Shahmohammadi, ISSCC 2015

Phase Noise

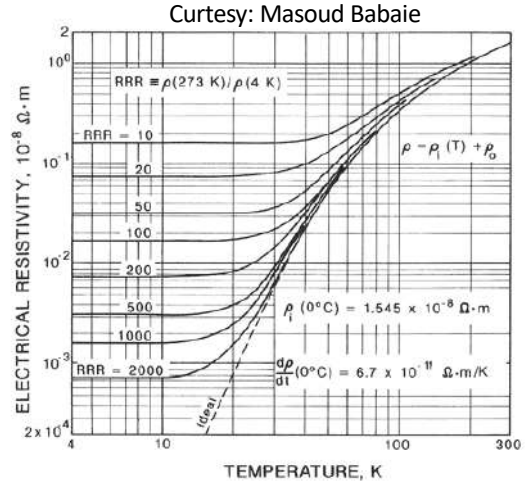


Measured Phase Noise



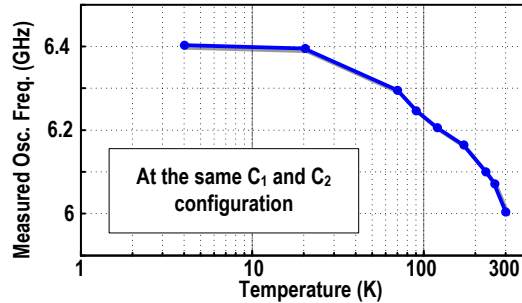
Sources of noise:

- Thermal noise
- Shot noise
- Impurities in copper



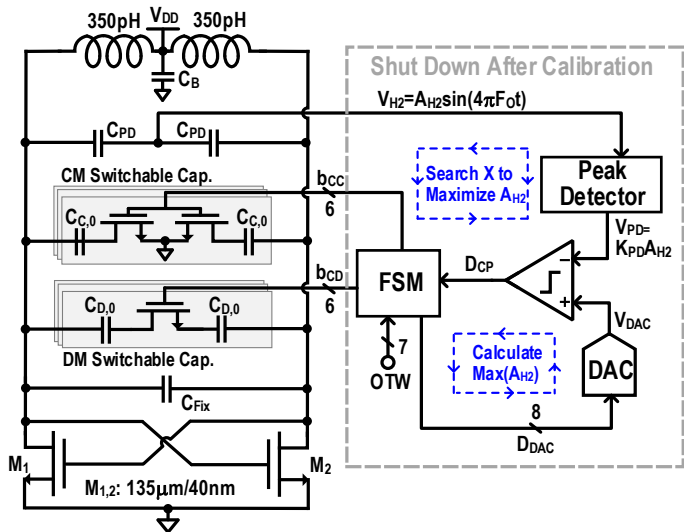
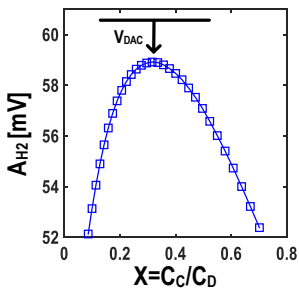
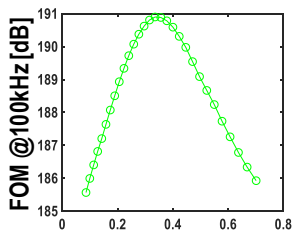
Source: copper.org

Frequency Stability

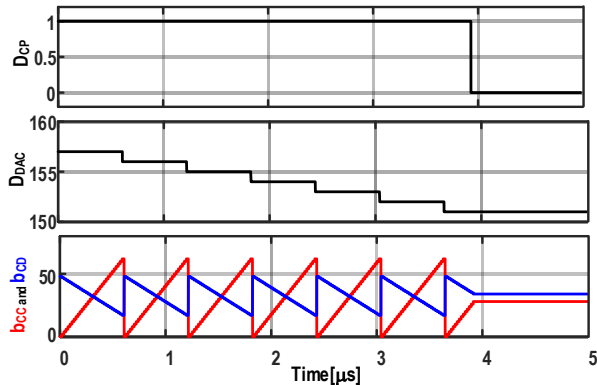
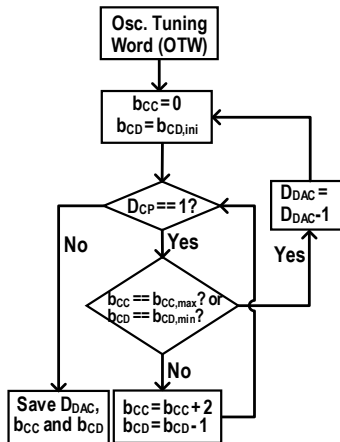


B. Patra et al, *JSSC* 2018

Improving Frequency Stability

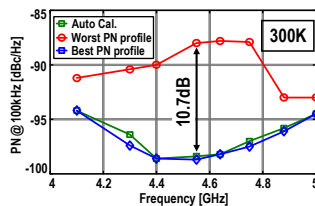
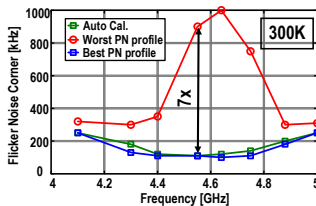
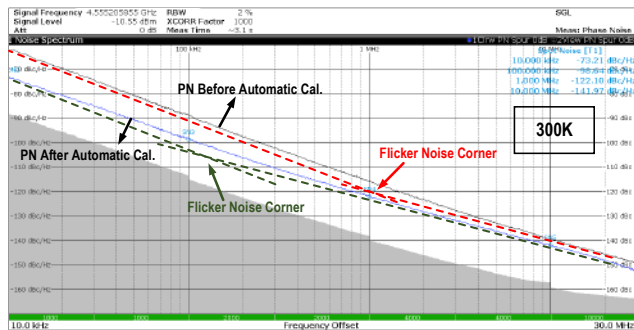


Improving Frequency Stability (2)



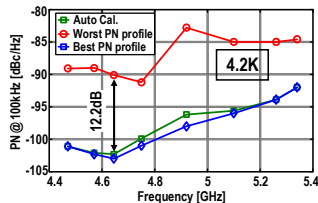
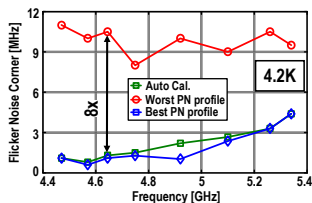
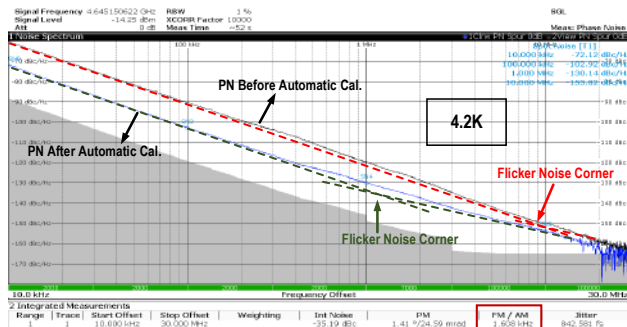
J. Gong, F. Sebastiano, E. Charbon, M. Babaie, *ISSCC 2020*

Phase Noise at 300K



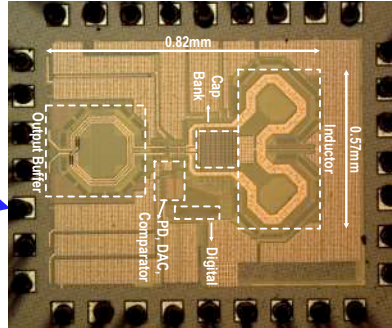
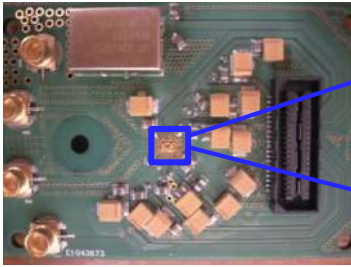
J. Gong, F. Sebastiano, E. Charbon, M. Babaie, *ISSCC* 2020

Phase Noise at 4K



J. Gong, F. Sebastiano, E. Charbon, M. Babaie, *ISSCC* 2020

Implementation in 40nm CMOS Node



Measurements at RT:

Technology: 40nm CMOS

F_{out} : 4.05-5.16GHz (24.1%)

F_{ref} : 20MHz

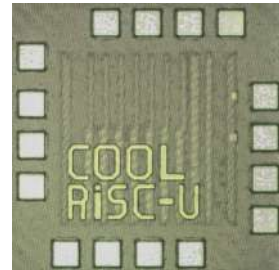
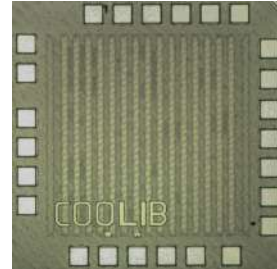
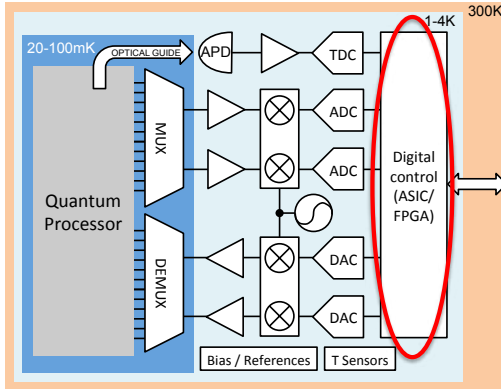
Supply: 0.5V (oscillator core)

Power consumption: 3.2mW

PN @10MHz: -141.5dBc/Hz

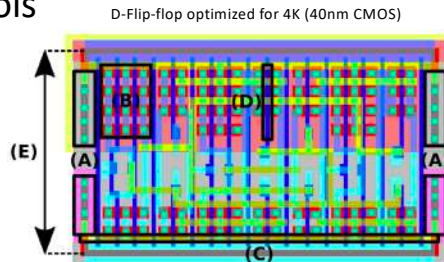
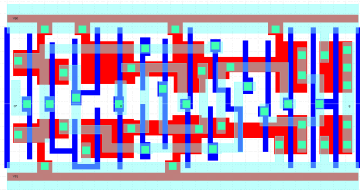
PN@100kHz: -98.8dBc/Hz

Cryo-Logic



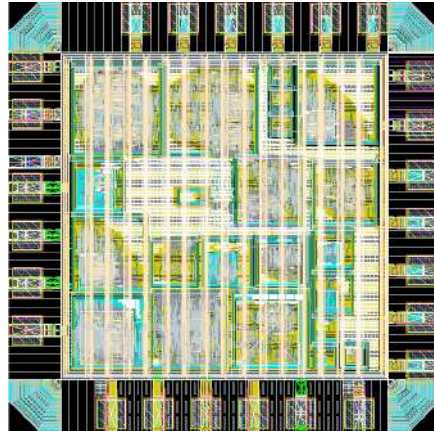
Ultra-Low Voltage Library 'cooLib'

- Digital library optimized for 4K
- Ultra low voltage operation (100s mV)
- Sub-threshold bias of N/P MOS
- Resilient to latchup and hysteresis-free
- Several logic families (static and dynamic CMOS)
- Compatible with commercial P&R tools



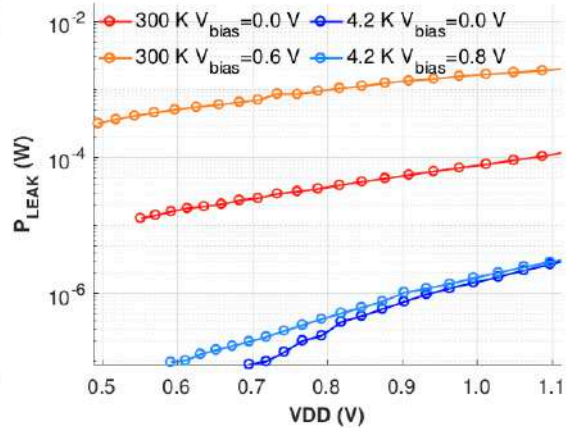
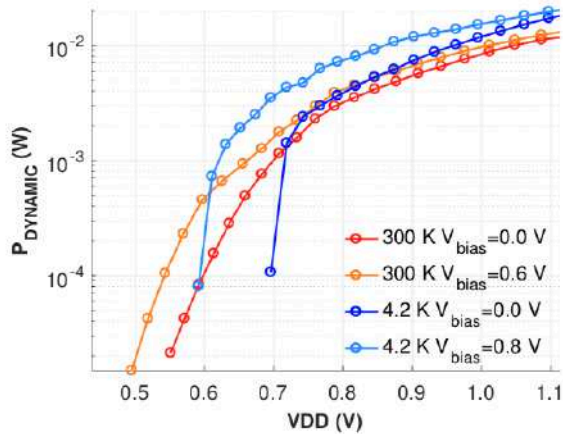
Test Chip Implementation

- Compare 'CooLib' cells to foundry supplied std. cells of TSMC40LP process
- Contains commonly encountered digital circuits
 - i.e. unsigned multiplier
- Four versions per circuit
 - Static 'CooLib'
 - Domino 'CooLib'
 - TSMC40LP, restricted
 - TSMC40LP, unrestricted
- One 'true' domino logic implementation

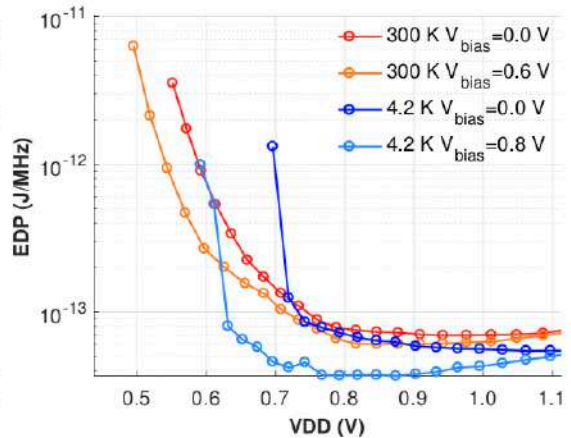
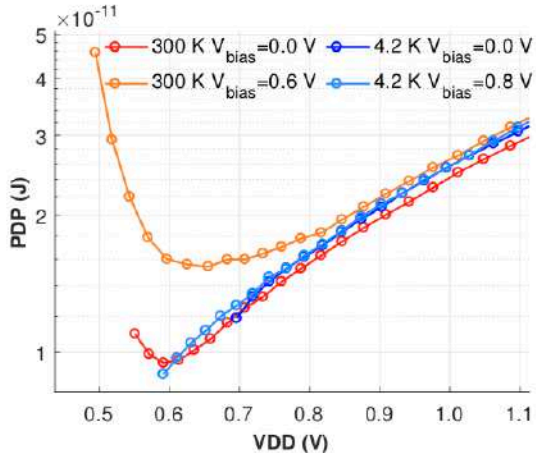


E. Schriek *et al.*, IEEE Solid-State Circuits Letters 2020

Dynamic vs. Static Power at Cryo



FOMs



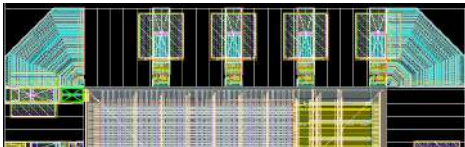
PDP: power-delay product
EDP: energy-delay product

Benchmarking

Benchmark	Temp.	$V_{DD,MIN}$ [V]			F_{MAX} @ 0.6 V [MHz]			F_{MAX} @ 0.7 V [MHz]			P_{AVG} @ 100 kHz [μW]		
		Proposed	A	B	Proposed	A	B	Proposed	A	B	Proposed	A	B
16X16 Multiplier	4.2 K	0.54	0.68	0.68	16.3	-	-	74.2	4.6	2.0	2.34	3.76	3.88
	300 K	0.3	0.49	0.44	100.4	9.7	17.4	145.2	34.0	39.7	0.61	2.68	1.92
EPFL Sine	4.2 K	0.58	0.68	0.68	1.95	-	-	20.9	2.2	1.1	3.91	4.00	4.46
	300 K	0.39	0.34	0.39	15.2	9.2	9.5	29.6	25.5	26.4	3.46	2.11	2.18
EPFL Int-to-Float	4.2 K	0.54	0.68	0.68	51.4	-	-	178.1	42.5	11.7	0.80	1.57	3.41
	300 K	0.24	0.38	0.36	118.5	75.2	73.44	174.2	191.9	158.0	0.08	0.55	0.28
EPFL Round-Robin Arbiter	4.2 K	0.58	0.68	0.68	21.6	-	-	46.6	2.0	1.8	7.89	11.56	11.64
	300 K	0.32	0.32	0.31	33.7	10.0	34.7	59.9	37.3	80.8	1.72	3.20	2.25

E. Schriek *et al.*, IEEE Solid-State Circuits Letters 2020

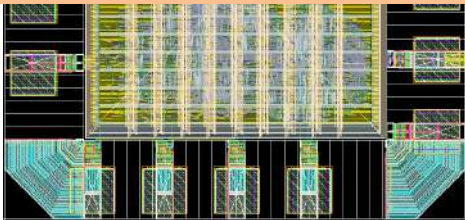
'CooLib' RISC-V Implementation



FEATURES

- RISC-V (picorv32, open-source) implemented using 'CooLib'

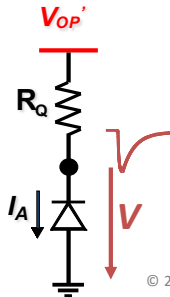
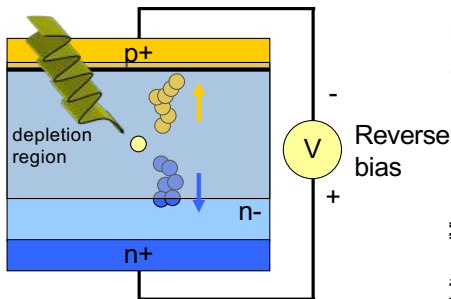
Fully functional μP operating at 4K



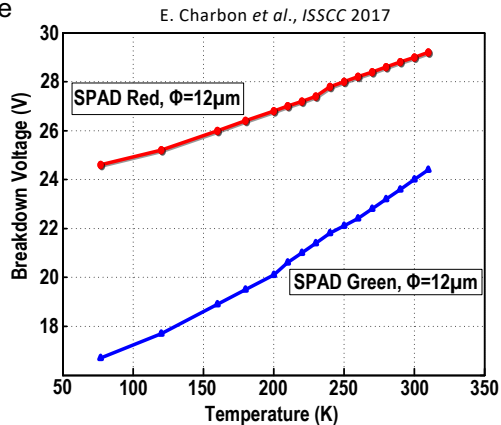
E. Schriek *et al.*, IEEE Solid-State Circuits Letters 2020

- Interfacing by 'CooLib' level-shifters
- UART interface for serial in/output
- JTAG interface for SRAM write/read

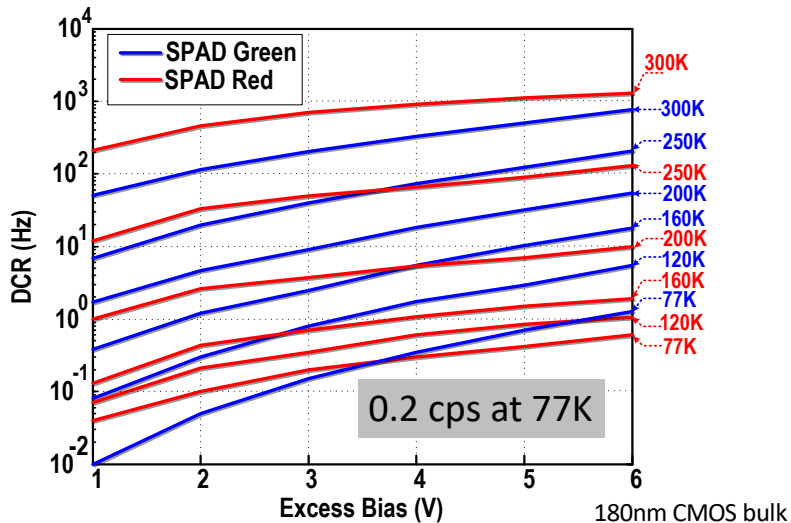
Cryo-Single-Photon APDs (Cryo-SPADs)



Operation in proportional and Geiger mode (SPAD)



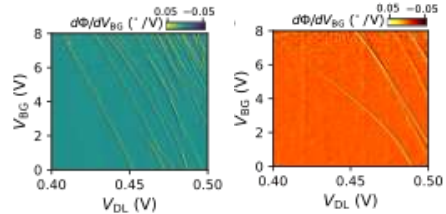
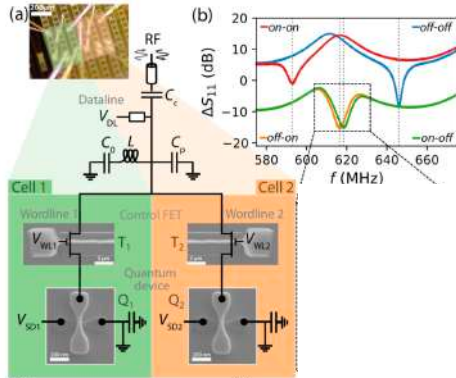
Cryo-SPADs



B. Patra *et al.*, JSSC 2018

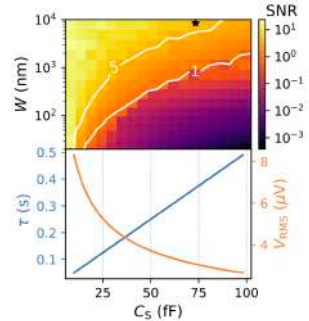
Qubits and Control in the Fridge

Step 1: Multiplexing Qubits



Two device gate maps measured in an interleaved manner

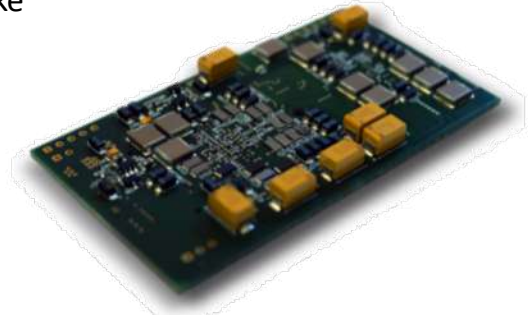
Approach can be applied down to 100nm scale



Step 2: Reading Qubits

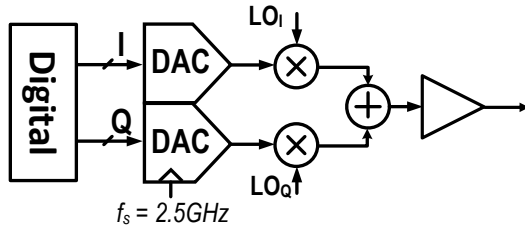
- **Single-shot dispersive readout**
- ***Single electron transistor*** readout
- (limited) use of 3D stacking
- Ideally bring qubits to 1-4K, make them CMOS-compatible

H. Homulle et al., QuRO interface
Silicon Quantum Electronics
Workshop, 2018

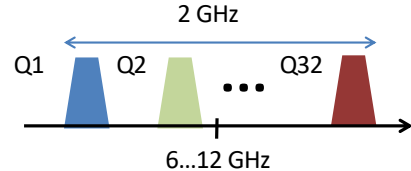


Step 3: Controlling Qubits

➤ Lower Speed DAC + Mixer



Analog: noise/linearity specifications known + feasible



Controlling Qubits: Specs

- Target fidelity: 99.99% for 1...10 MHz operation

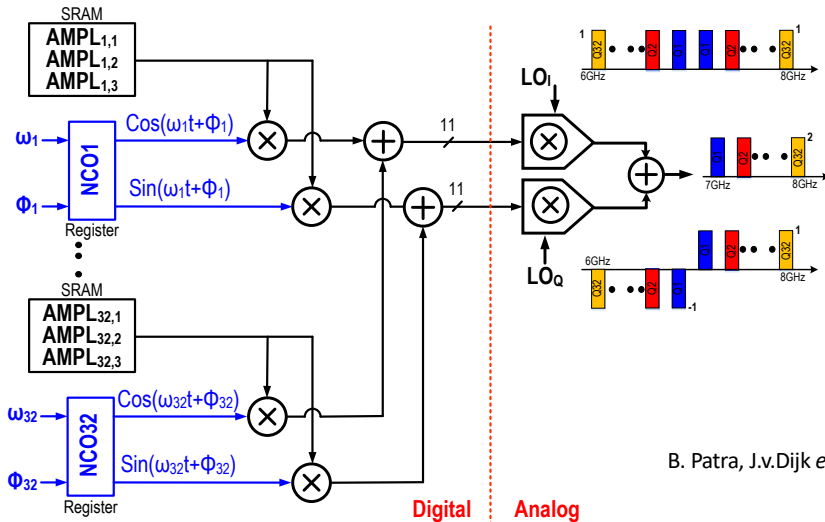
- Analog:

Error Source	Type	Value	Contribution
Microwave frequency (nominally 5...13 GHz)	inaccuracy	35.4 kHz	1-F = 12.5 ppm
	noise	35.4 kHz _{rms}	1-F = 12.5 ppm
Microwave phase	inaccuracy	0.20 °	1-F = 12.5 ppm
	noise	0.20 °	1-F = 12.5 ppm
Microwave amplitude (nominally 17 mV, -53 dB)	inaccuracy	38.3 μV	1-F = 12.5 ppm
	noise	38.3 μV _{rms}	1-F = 12.5 ppm
Microwave duration (nominally 50 ns)	inaccuracy	113 ps	1-F = 12.5 ppm
	noise	113 ps _{rms}	1-F = 12.5 ppm

+

$F = 99.99\%$

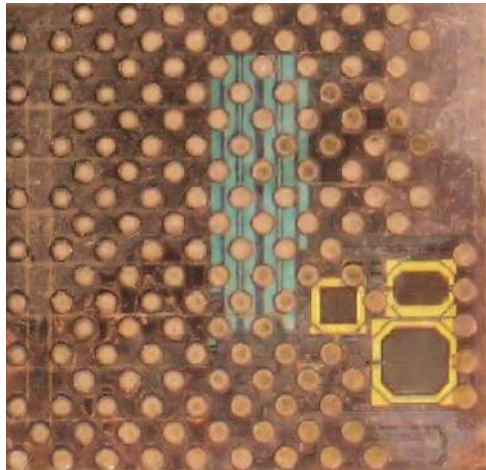
Controller Architecture: Horse Ridge



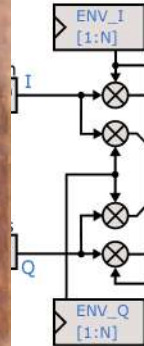
B. Patra, J.v.Dijk *et al.*, ISSCC 2020

Controller Implementation

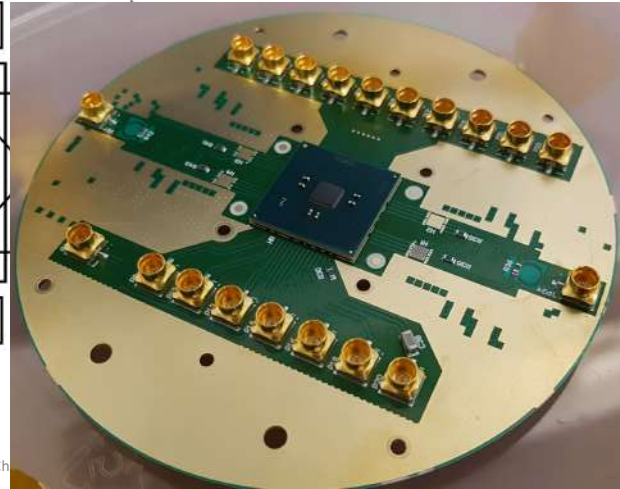
B. Patra, J.v.Dijk *et al.*, ISSCC 2020



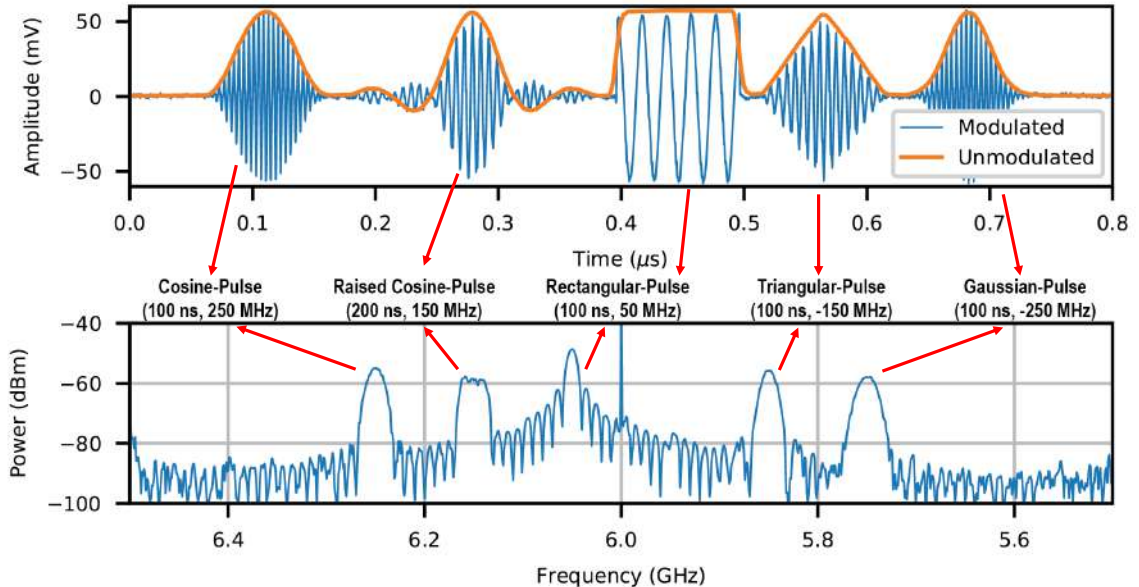
DIGITAL
MODULATION



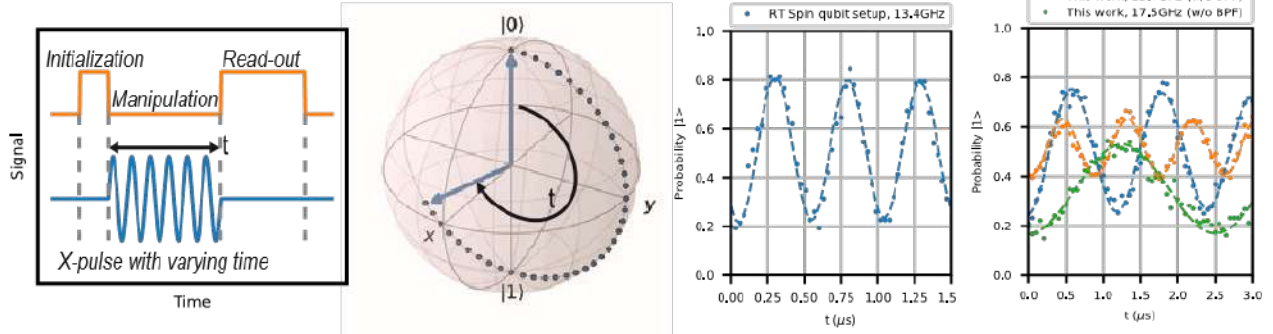
ANALOG
DAC/Filter/Mixer



Pulse Shaping

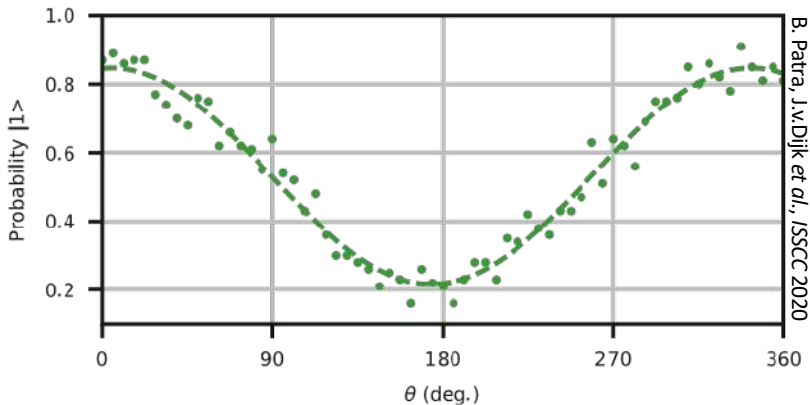
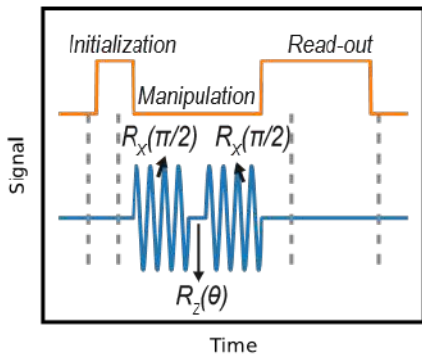
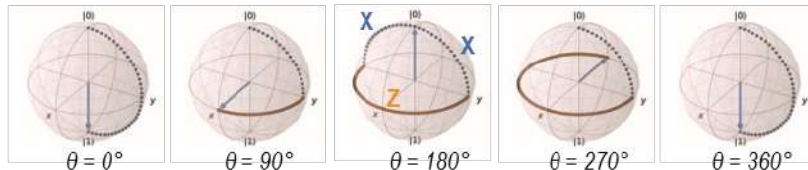
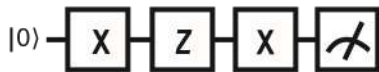


Rabi Experiment



B. Patra, J.v.Dijk *et al.*, ISSCC 2020

Qubit Manipulation



B. Patra, J.v.Dijk et al., ISSCC 2020

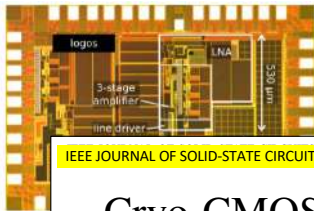
Comparison Table

	Horse Ridge (ISSCC'20)	ISSCC'19	RSI'17	Spin qubit setup
Operating Temperature	3 K	3 K	300 K	300 K
Qubit platform	Spin qubits + Transmons	Transmons	Transmons	Spin qubits
Qubit frequency	2 – 20 GHz	4 – 8 GHz		< 20 GHz
Channels	128 (32 per TX)	1	4	1
FDMA	Yes, SSB	No	Yes, SSB	No
Data Bandwidth	1 GHz	400 MHz	960 MHz	520 MHz
Image & LO leakage calibration	On chip	Off chip	Yes	
Phase correction	Yes	No	No	No
Fidelity (expected)	99.99%	-	-	-
Waveform/Instructions	Upto 40960 pts AWG	Fixed 22 pts symmetric		16M pts AWG
Instruction set	Yes	No	Yes	Yes
Power / TX	Analog: 1.7 mW/qubit * Digital: 330 mW ‡	Analog < 2 mW/qubit # Digital: N/A		850 W
Chip area / TX	4 mm ²	1.6 mm ²	Discrete	Rack mount
Technology	22 nm FinFET CMOS	28 nm bulk CMOS	components	

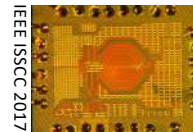
* including LO/Clock driver; only RF-Low active # does not mention circuits included

‡ can be reduced with clock gating

In Summa



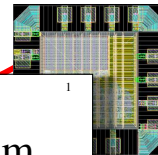
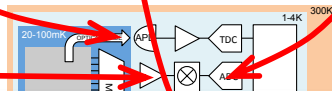
IEEE IEDM 2016



IEEE ISSCC 2017



IEEE IEDM 2016

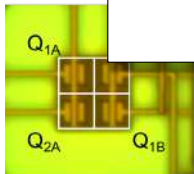


IEEE JOURNAL OF SOLID-STATE CIRCUITS

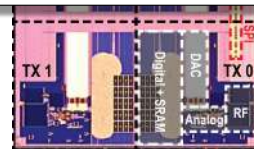
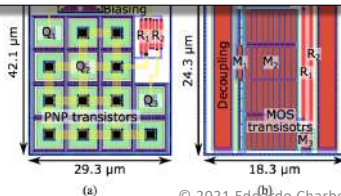
1

Cryo-CMOS Circuits and Systems for Quantum Computing Applications

Bishnu Patra, *Student Member, IEEE*, Rosario M. Incandela, *Student Member, IEEE*, Jeroen P. G. van Dijk, Harald A. R. Homulle, Lin Song, Mina Shahmohammadi, *Member, IEEE*, Robert Bogdan Staszewski, *Fellow, IEEE*, Andrei Vladimirescu, *Fellow, IEEE*, Masoud Babaie, *Member, IEEE*, Fabio Sebastiano, *Senior Member, IEEE*, and Edoardo Charbon, *Fellow, IEEE*



IEEE Sensors 2016



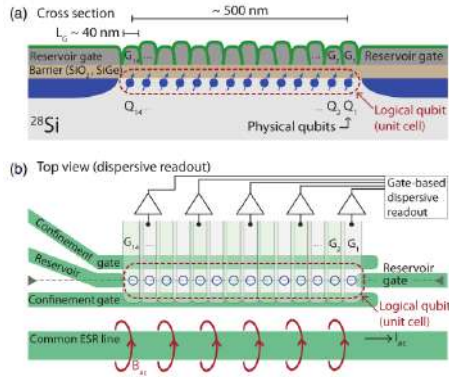
IEEE ISSCC 2020



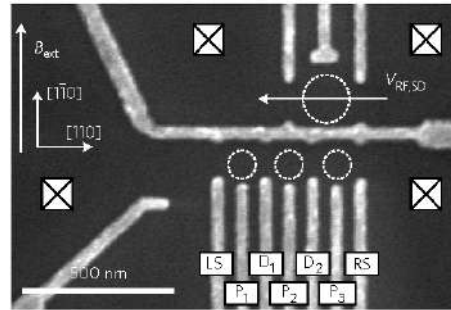
ISSCC 2020

5. Conclusions

Realizations of 1D Qubit Arrangements

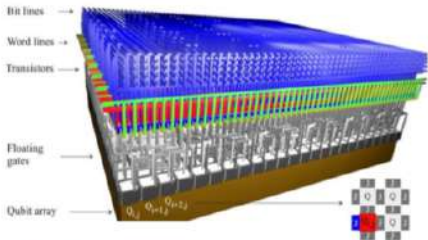
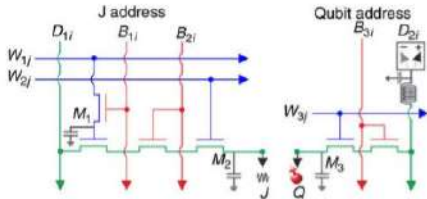


Jones *et al*, PRX 8, 021058 (2018)

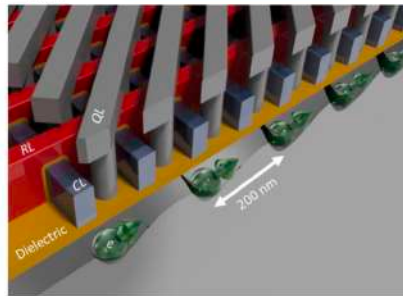
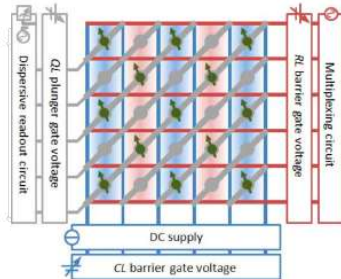


Baart *et al*, Nat Nano (2017)

Proposals for Scalable Fault-Tolerant 2D Qubit Arrangements



**M. Veldhorst et al. (UNSW),
Nature Comm. (2017)**

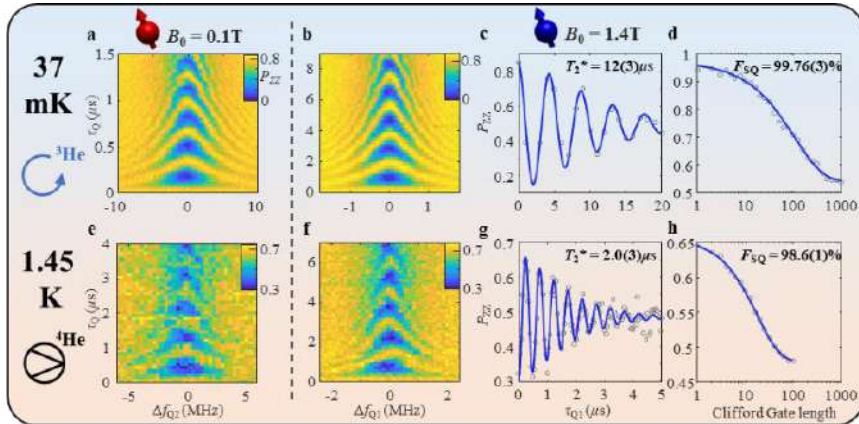


R. Li et al., arXiv 1711.03807 (2017)

SiMOS QD Qubit Operation at 1.5 Kelvin

Silicon quantum processor unit cell operation above one Kelvin

C. H. Yang,^{1,*} R. C. C. Leon,¹ J. C. C. Hwang,^{1,†} A. Saraiva,¹ T. Tanttu,¹
W. Huang,¹ J. Camirand Lemyre,² K. W. Chan,^{1,‡} K. Y. Tan,^{1,‡} F. E. Hudson,¹
K. M. Itoh,³ A. Morello,¹ M. Pioro-Ladrière,^{2,4} A. Laucht,¹ and A. S. Dzurak^{1,§}

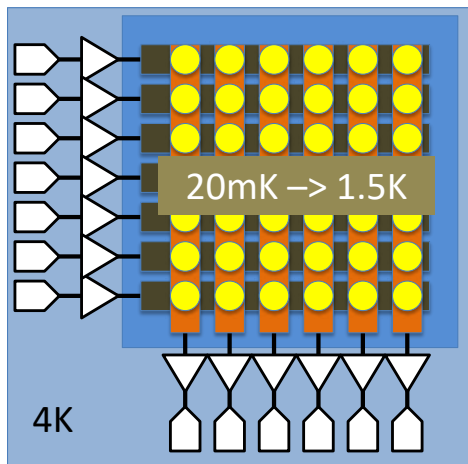


\Rightarrow 1.5 K performance comparable to natSi at 100 mK !

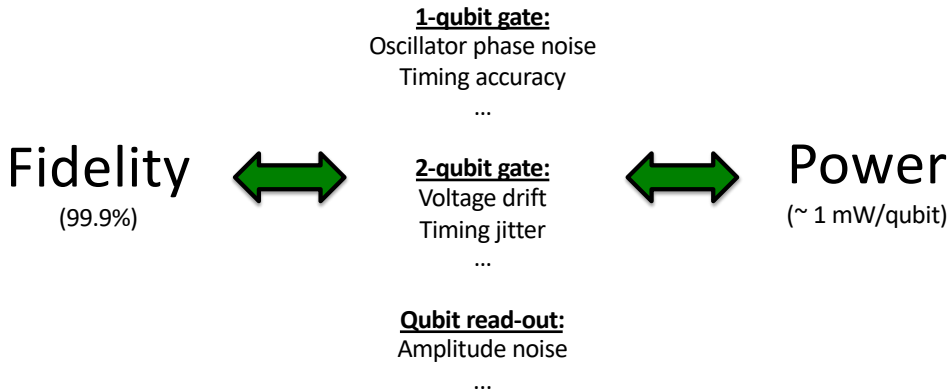
Courtesy: A. Dzurak

Platforms for the 2D Approach

- **Single-shot dispersive readout** could be the core of column readouts
- Use ***imaging sensor*** readout as inspiration
- Use tunneling barriers as selectors
- (limited) use of 3D stacking
- Ideally bring qubits to 1-4K, make them CMOS-compatible



Tradeoffs



- Fidelity is usually expressed as a percentage, often referred to as x9's (e.g. 5 9's = 99.999%)
- Higher fidelity usually requires high power, which is budgeted, especially at low temperatures (e.g. μW of thermal absorption at mK, while W at 4K)

Quantum Computing

- A quantum computer is a new computing paradigm and as such it holds the promise to handle today's intractable problems
- A qubit is fragile and thus needs to be constantly corrected to extend its coherence and to maintain fidelity
- Cryogenic electronics for quantum computing ensures compactness and scalability to much larger quantum processors

IceQubes: International Workshop on Cryogenic Electronics for Quantum Systems

June 2021, Neuchâtel - Switzerland

